Geochemistry Geophysics Geosystems G3

Article
Volume 12, Number 6
28 June 2011
Q06018, doi:10.1029/2011GC003508
ISSN: 1525-2027

Published by AGU and the Geochemical Society

Three-dimensional model of an ultramafic feeder system to the Nikolai Greenstone mafic large igneous province, central Alaska Range

Jonathan M. G. Glen
U.S. Geological Survey, Menlo Park, 345 Middlefield Rd., MS989, California 94025, USA (jglen@usgs.gov)

Jeanine M. Schmidt
U.S. Geological Survey, 4210 University Dr., Anchorage, Alaska 99508-4626, USA

Gerry G. Connard
Geosoft Inc., 1600 SW Western Blvd., Ste. 250, Corvallis, Oregon 97333-4122, USA

[1] The Amphitheater Mountains and southern central Alaska Range expose a thick sequence of Triassic Nikolai basalts that is underlain by several mafic-ultramafic complexes, the largest and best exposed being the Fish Lake and Tangle (FL-T) mafic-ultramafic sills that flank the Amphitheater Mountains synform. Three-dimensional (3-D) modeling of gravity and magnetic data reveals details of the structure of the Amphitheater Mountains, such as the orientation and thickness of Nikolai basalts, and the geometry of the FL-T intrusions. The 3-D model (50 × 70 km) includes the full geographic extent of the FL-T complexes and consists of 11 layers. Layer surfaces and properties (density and magnetic susceptibility) were modified by forward and inverse methods to reduce differences between the observed and calculated gravity and magnetic grids. The model suggests that the outcropping FL-T sills are apparently connected and traceable at depth and reveals variations in thickness, shape, and orientation of the ultramafic bodies that may identify paths of magma flow. The model shows that a significant volume (2000 km^3) of ultramafic material occurs in the subsurface, gradually thickening and plunging westward to depths exceeding 4 km. This deep ultramafic material is interpreted as the top of a keel or root system that supplied magma to the Nikolai lavas and controlled emplacement of related magmatic intrusions. The presence of this deep, keel-like structure, and asymmetry of the synform, supports a sag basin model for development of the Amphitheater Mountains structure and reveals that the feeders to the Nikolai are much more extensive than previously known.

Components: 10,100 words, 16 figures, 2 tables.

Keywords: Amphitheater Mountains, south central Alaska; Nikolai flood basalt; Wrangellia; gravity; magnetics; three-dimensional geophysical model.

Index Terms: 0920 Exploration Geophysics: Gravity methods (1219); 0925 Exploration Geophysics: Magnetic and electrical methods (5109); 8137 Tectonophysics: Hotspots, large igneous provinces, and flood basalt volcanism.

Received 10 January 2011; **Revised** 8 April 2011; **Accepted** 11 April 2011; **Published** 28 June 2011.

Glen, J. M. G., J. M. Schmidt, and G. G. Connard (2011), Three-dimensional model of an ultramafic feeder system to the Nikolai Greenstone mafic large igneous province, central Alaska Range, *Geochem. Geophys. Geosyst.*, *12*, Q06018, doi:10.1029/2011GC003508.

Copyright 2011 by the American Geophysical Union

1. Introduction

[2] One of the most complete sections of a large igneous province (LIP) worldwide is in the Amphitheater Mountains, Alaska (Figure 1) where a near-continuous section from basal gabbroic sills and submarine-to-subaerial basalts of the Nikolai Greenstone Formation is exposed. Abundant mafic-to-ultramafic (MUM) intrusions in the Amphitheater Mountains and southern Alaska Range to the north and east suggest that this area was a primary vent site for Nikolai LIP volcanism. Two of the MUM intrusions, the cyclically layered and compositionally graded Fish Lake (also referred to as the Alpha) complex and the Tangle (also referred to as the Beta) complex, as well as their sedimentary host units, form the asymmetrical Amphitheater synform beneath the thickest exposures of the Nikolai flood basalts.

[3] This study models the structure of the Amphitheater synform and adjacent areas in 3-D to better constrain its geometry, lend insight into how it formed, and provide more accurate estimates of the volumes of Nikolai basalts and related ultramafic sills, which are relevant to determining the area's mineral potential. Distinct density and magnetic properties of the Nikolai basalts, and ultramafic and sedimentary rocks make the synform particularly amenable to potential field (magnetic and gravity) modeling.

[4] Goals of the modeling were (1) to distinguish between postextrusive (syncline) and synvolcanic (sag basin) models for formation of the Amphitheater Mountains structure, (2) to determine the volumes of Nikolai lavas and ultramafic rocks within the synform, (3) to help resolve spatial relationships between the Fish Lake and Tangle intrusions and nearby ultramafic bodies (Canwell, Eureka, Rainy) which have been interpreted as other segments of the Nikolai LIP, and address the "magmatic connectivity" of these complexes, (4) to assess the role of synvolcanic structural controls on the emplacement of the Nikolai magmatic system and the size, shape, and location of magma chambers (mafic-ultramafic complexes); and (5) to possibly identify shallow, drill-accessible portions of ultramafic intrusions that could host prospective Ni-Cu ± PGE magmatic sulfide deposits.

1.1. Wrangellia Terrane Overview

[5] South central Alaska consists of Paleozoic to Mesozoic tectonostratigraphic terranes (Figure 1b) accreted to North America during Jurassic to Cretaceous subduction. The lithostratigraphic terrane underlying the Amphitheater Mountains is Wrangellia, a sequence of Mississippian to Middle Triassic metasedimentary and metavolcanic rocks characterized by extensive flood basalts of the Middle to Late Triassic Nikolai Greenstone, overlain by Triassic and Jurassic shallow marine sedimentary rocks, and cut by Nikolai-related gabbroic, ultramafic, and dolerite sills [*Nokleberg et al.*, 1994].

[6] Wrangellia and other intraoceanic terranes in south central Alaska [*Berg et al.*, 1972; *Jones et al.*, 1972; *Berg et al.*, 1978; *Plafker and Berg*, 1994; *Nokleberg et al.*, 1994] were accreted to the continental margin as subduction-related convergence closed a series of intervening marginal seas. Wrangellia was likely well south (~30° latitude) of its present position during extrusion of the Nikolai in Middle to Late Triassic time [*Hillhouse and Coe*, 1994]. Following accretion, it was splintered, and some segments moved northward by oblique translation along coast-parallel strike-slip systems. The assembled southern Alaska terranes were locally stitched by Mid-Cretaceous and Tertiary plutons and volcanic fields and cut by Cenozoic to Recent strike slip and thrust fault systems such as the Hines Creek and McKinley strands of the Denali Fault Zone.

[7] Wrangellia in the study area, contains a different pre-Nikolai stratigraphy than at its type section in the Wrangell Mountains (Figure 3a) [e.g., *Werdon et al.*, 2001; *Schmidt et al.*, 2003; *Greene et al.*, 2010]. Amphitheater Mountain Nikolai basalts are underlain by fine-grained argillites and shales of Permian to Triassic age, which are variably intruded by gabbroic sills interpreted as feeders to the Nikolai Greenstone. Pennsylvanian to Permian volcaniclastic and volcanic rocks (e.g., Tetelna Formation) more characteristic of the type section of Wrangellia are limited to the northeastern part of the study area, outside of the Amphitheater synform. These two stratigraphies were interpreted as the Tangle and Slana River subterranes, respectively, by *Nokleberg et al.* [1992].

[8] Minor post-Nikolai calcareous and argillaceous rocks of Late Triassic age (assigned to the Clearwater terrane of *Nokleberg et al.* [1992]) are exposed in the study area between Wrangellia and the Maclaren metasediments. Some sills and basalts of the Amphitheater Nikolai sequence yield $^{40}Ar/^{39}Ar$ ages of plagioclase (160–169 Ma) suggestive of thermal resetting by Middle Jurassic plutons which

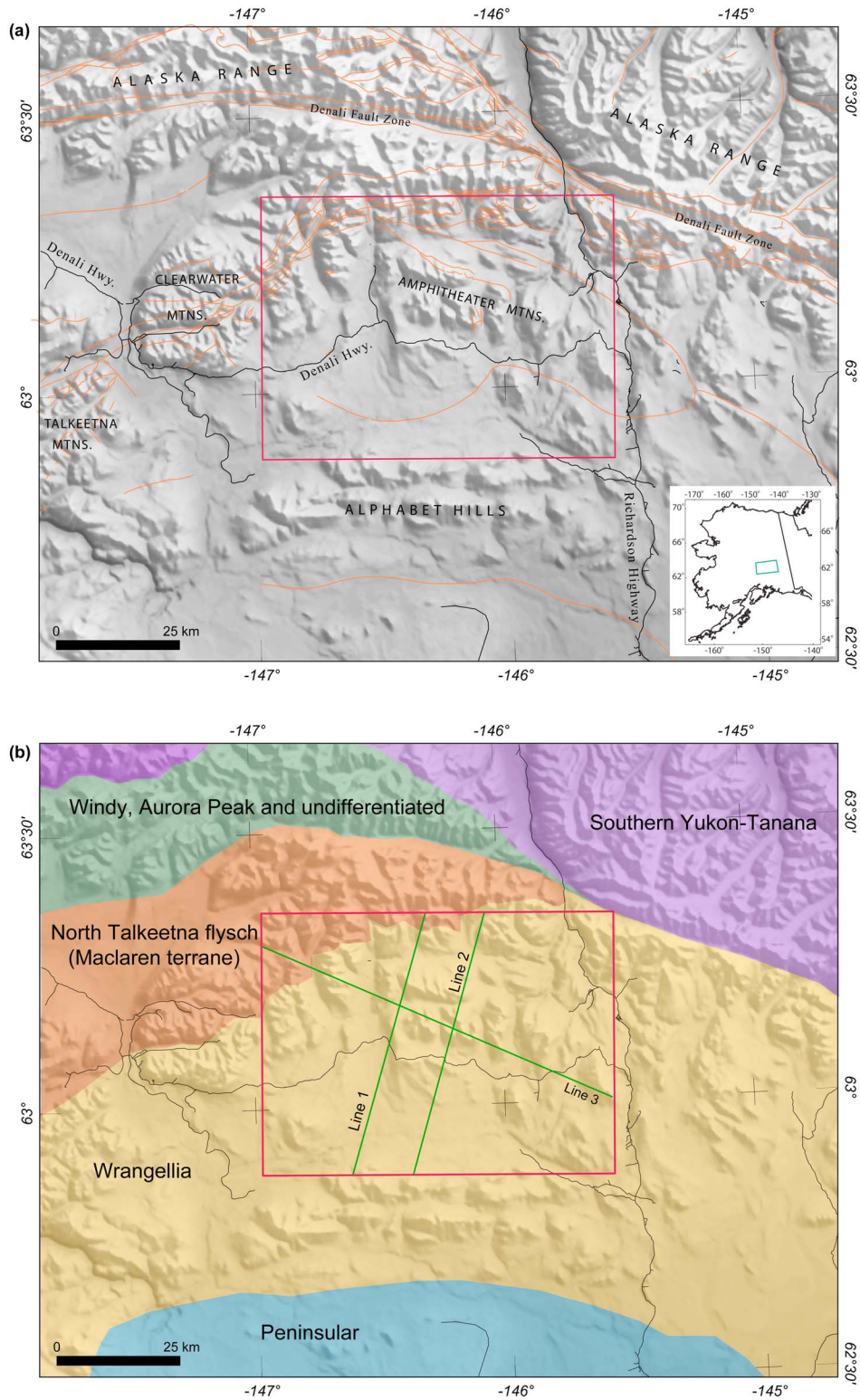

Figure 1. (a) Digital shaded relief map of the Amphitheater Mountains and surrounding region, south central Alaska showing physiographic features, roads and trails (black lines), and mapped faults (orange lines [*Nokleberg et al.*, 1992]). The red box outlines the 3-D model area (area of Figures 2a and 2b). (b) Major tectonostratigraphic terranes in the Amphitheater Mountains and surrounding region, south central Alaska [after *Glen et al.*, 2007a]; terrane-bounding faults are a subset of those indicated in Figure 1a. The red box outlines the 3-D model area (area of Figures 2a and 2b). Green lines show the locations of profile lines 1, 2, and 3 that were extracted from the 3-D model.

intrude Wrangellia southwest of the study area [*Greene et al.*, 2010].

[9] A series of Jurassic-Cretaceous flysch basins developed as overlap assemblages inboard of the leading margin of Wrangellia during suturing [*Eastham and Ridgway*, 2002; *Ridgway et al.*, 2002; *Trop et al.*, 2002]. Remnants of one flysch sequence, the Maclaren unit in the northwest part of the study area (Figures 1 and 2), include metamorphosed fine-grained clastic rocks of unknown provenance, intruded by Late Cretaceous to Tertiary plutons (the Maclaren terrane and East Susitna Batholith of *Nokleberg et al.* [1992]). Maclaren metasediments are thrust southward over Wrangellia along the Broxson Gulch and related thrust faults and are truncated to the north by the McKinley strand of the Denali fault.

1.2. Nikolai Large Igneous Province

[10] The term "large igneous province" (LIP) refers to continental or oceanic flood basalt eruptions [*Coffin and Eldholm*, 1994] typically with areal extents exceeding 100,000 km^2, in which large volumes (>100,000 km^3) of mafic magma erupted over a relatively short period of time (commonly >75% erupted in 1–5 Myr [*Bryan and Ernst*, 2008]). They are often ascribed to the ascent and impact of a mantle plume on the lithosphere which, accompanied by rifting, leads to ensuing eruptions. Wide variations in magma type, tectonic setting, duration of magmatism, etc., of different LIP provinces, however, suggests that a variety of mechanisms, rather than a single (plume) model, may be required to explain the origin and evolution of different LIPs [*Bryan and Ernst*, 2008].

[11] Regardless of their ultimate origin, mechanisms of magma emplacement at middle to shallow crustal depths and magma venting are likely similar in many LIPs. The eruptive histories, the number and geometry of vents, and the role of structure, stratigraphy, and tectonics in controlling magmatic pathways for LIPs, are poorly understood because few root systems or midcrustal levels of LIPs are exposed worldwide. Studies of vent geometries and their structural and tectonic settings may shed light on LIP origins (e.g., plume versus rift or back-arc models), help predict the locations of possible vent areas, and aid in assessing the relative importance of crustal heterogeneity, stress fields, and preexisting structural grain on magma emplacement. This is the scope of the present study which focuses on the Middle to Late Triassic Nikolai Greenstone–one of the oldest (~230 Ma) and best exposed flood basalt events preserved in the world.

[12] The Nikolai flood basalts (sometimes referred to as the Wrangellia flood basalts) formed as an oceanic plateau basalt province [*Panuska*, 1990; *Ernst and Buchan*, 2001] near a continental margin, perhaps in a back-arc–island arc setting [*Nokleberg et al.*, 1994]. Although controversy remains over whether Nikolai petrochemistry suggests a mantle plume [*Richards et al.*, 1991; *Lassiter et al.*, 1995] or back-arc rifting [*Barker et al.*, 1989] origin, most oceanic plateaus of Nikolai scale are explained by mantle plume sources [*Kerr and Mahoney*, 2007]. Recent geochemical data from the Nikolai lavas suggest a plume-type Pacific mantle source similar to that of basalts from the Ontong Java and Caribbean plateaus [*Greene et al.*, 2009].

[13] The Nikolai volcanic province is one of the 20 largest LIPs worldwide (estimated at ~1 × 10^6 km^3). Its remnants are preserved along more than 2,500 km of the western North American margin from south central Alaska to British Columbia and Vancouver (Figure 3). The original shape of the Nikolai flood basalt province is difficult to determine; its present ribbon-shaped distribution of fragments results from a long history of oblique accretion and margin-parallel strike-slip faulting [*Jones et al.*, 1977].

[14] Paleozoic rocks of the Wrangellia terrane were deposited in settings ranging from continental margins to island arcs (Figure 4). Nikolai basalts in south central Alaska were extruded primarily over Mississippian to Triassic siliceous argillite, siltstone, chert and limestone, rather than Pennsylvanian-Permian volcanic rocks as seen at the Nikolai type section in the Wrangell Mountains. Nikolai basalts have undergone metamorphism ranging from very low grade (zeolite facies, in the Amphitheater Mountains) to greenschist facies (most exposures). Gabbro sills intrude the base of the volcanic pile in the Amphitheater Mountains and the sedimentary section immediately below it. Basal Nikolai lavas (~500 m of section) in the Amphitheater Mountains [*Greene et al.*, 2008] are submarine, while the majority of the 3.5–4 km thick Nikolai section there was erupted subaerially [*Greene et al.*, 2008], suggesting relatively shallow water depths for initial emplacement and emergence through a combination of uplift (?) and infill of the submarine basin.

[15] Nikolai flood basalts, like many other LIPs, probably erupted over a relatively short period of time. Ladinian (late Middle Triassic) bivalves are preserved in argillaceous sedimentary rocks imme-

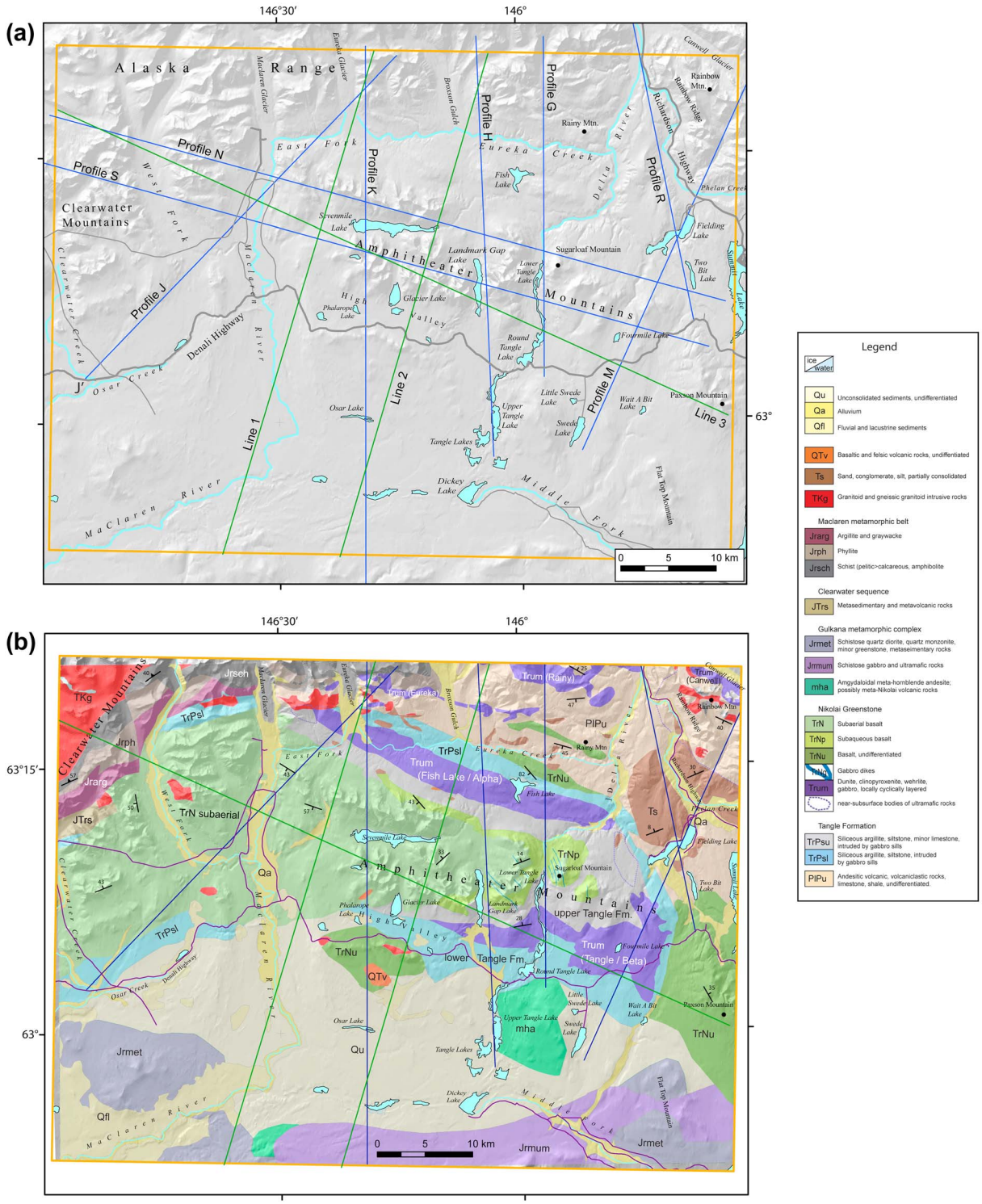

Figure 2. (a) Digital shaded relief map of the 3-D model area (orange box) showing physiographic features, major roads (gray lines), rivers and lakes (light blue). Dark blue lines (profiles G, H, J, K, L, M, N, R, and S) show the locations of 2-D profile models that were used to construct the initial 3-D model. Green lines (lines 1–3) show 2-D model profiles extracted from the 3-D model. (b) Geologic map of the 3-D model area (orange box in Figure 2a). Map compiled from *Nokleberg et al.* [1992]; *Greene et al.* [2010]; unpublished mapping of NevadaStar, Inco, and USGS; and interpretations of magnetic and gravity data. Green and dark blue lines are model profiles shown and labeled in Figure 2a.

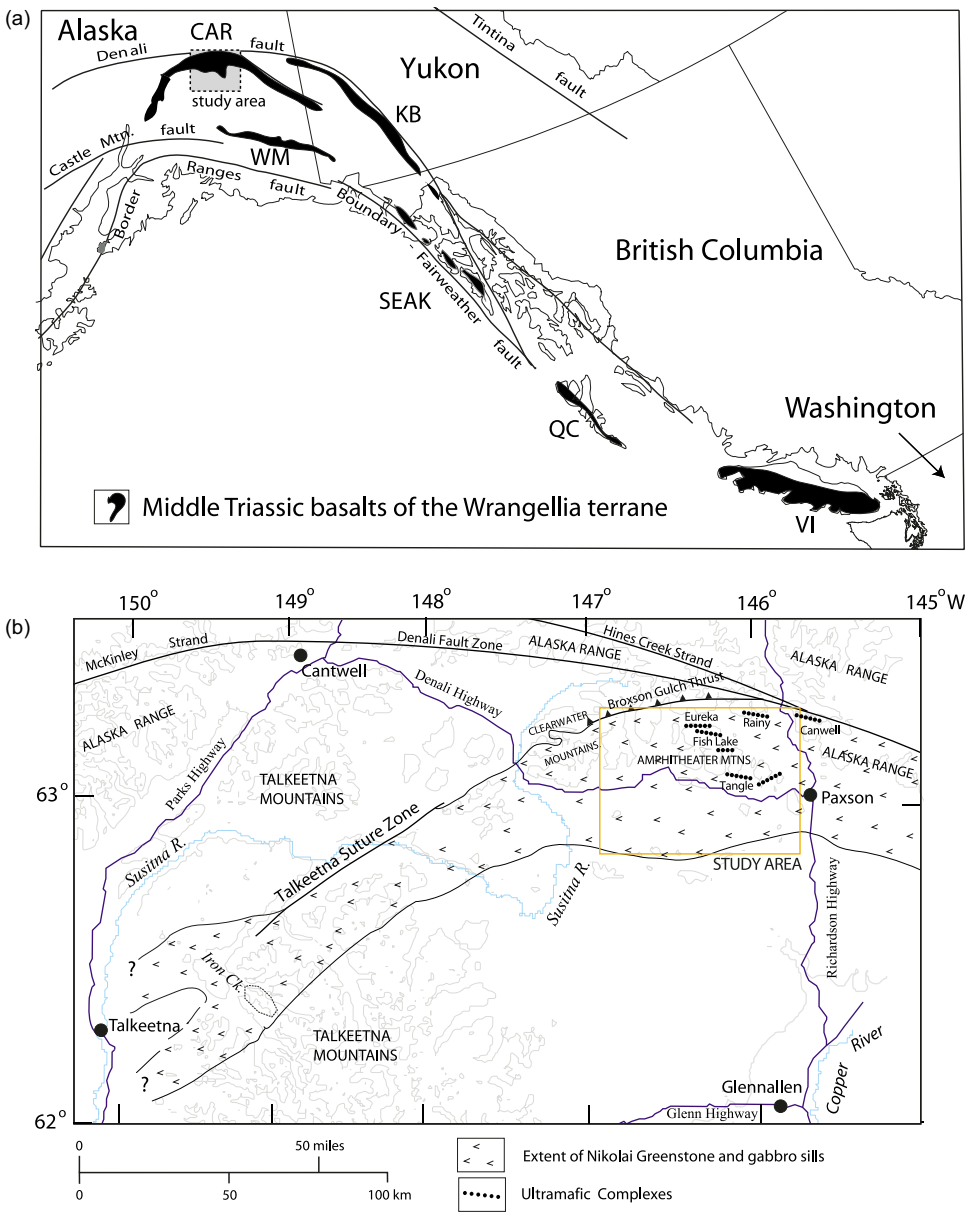

Figure 3. (a) Map showing distribution of Nikolai Greenstone and correlative basalts along western North American margin (adapted from *Jones et al.* [1977]). VI, Vancouver Island; WM, Wrangell Mountains; SEAK, southeast Alaska; QC, Queen Charlotte Islands; KB, Kluane Belt; CAR, Central Alaska Range. Dashed box indicates the approximate bounds of the study area. (b) Map of south central Alaska showing extent of Nikolai Greenstone and related sill complexes, 3-D model area (orange box), topographic contours (gray lines), roads (dark blue lines), rivers (light blue lines), and faults (thick black lines).

diately below the Nikolai at its type section in the Wrangell Mountains and on Vancouver Island [*Greene et al.*, 2010]. Sparse Middle or Late Triassic bivalves in argillite are interbedded with basal pillowed Nikolai in the study area [*Nokleberg et al.*, 1992]. Late Carnian to early Norian (early Late Triassic) fossils are found in limestones immediately overlying the Nikolai at the type section and in the Talkeetna Mountains [*Jones et al.*, 1977; *Schmidt et al.*, 2003]. Radiometric ages ($^{40}Ar/^{39}Ar$ and U–Pb) of peridotite and gabbro intrusions interpreted as feeders to the Nikolai in Yukon and central Alaska, and $^{40}Ar/^{39}Ar$ ages of basalts from the Wrangell Mountains, range from 227 to 232 Ma [*Lassiter et al.*, 1995; *Bittenbender et al.*, 2007; *Schmidt and Rogers*, 2007; *Greene et al.*, 2010],

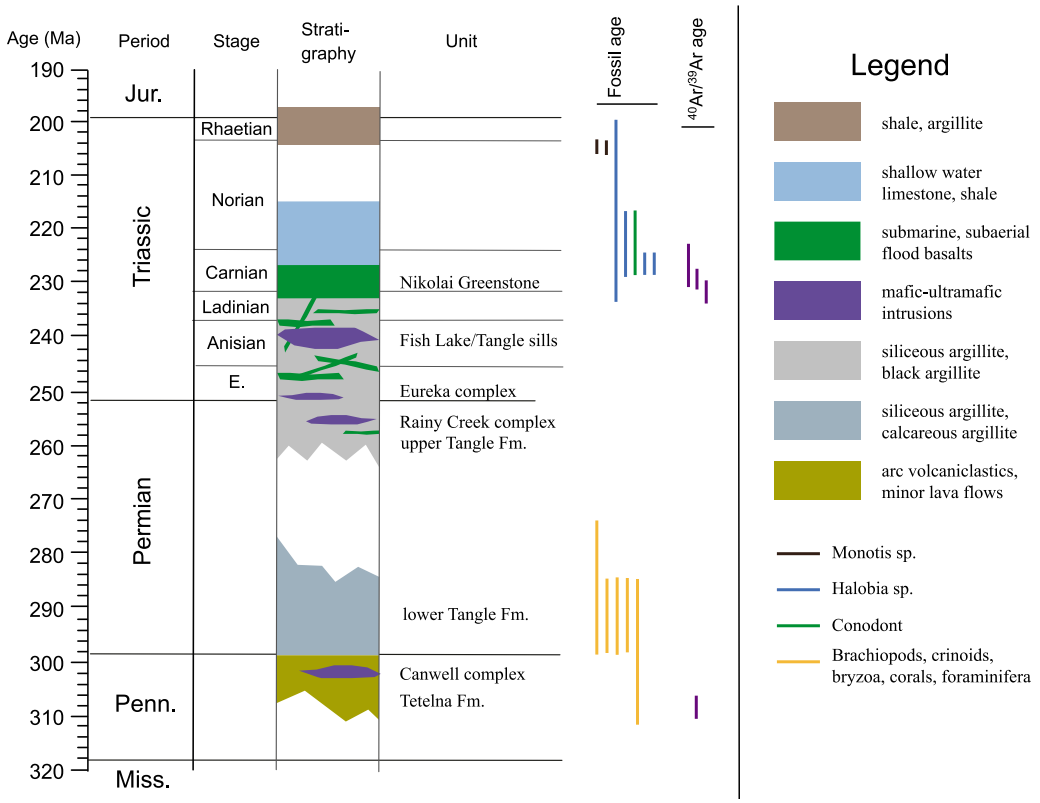

Figure 4. Generalized stratigraphic column and age control of Nikolai-related rocks within the Central Alaska Range belt. Time scale shown is that of *Gradstein and Ogg* [2004]. Fossil and isotopic age data are summarized in Supplemental Data File 5 of *Greene et al.* [2010]. Figure is modified after *Schmidt and Rogers* [2007, Figure 3].

indicating a Middle–Late Triassic age for the Nikolai, and suggesting that the bulk of the province may have been emplaced in only a few million years.

1.3. Amphitheater Mountains: Geology

[16] The Amphitheater Mountains, study area, located north of the Copper River basin, form a topographic outlier to the Alaska Range that lies immediately to the north and northeast (Figure 1). Several MUM intrusive complexes are exposed in the study area; all are interpreted as parts of the Nikolai LIP magmatic system. The two largest MUM complexes, the Fish Lake and Tangle (Figures 2 and 5) occur along the northern and southeastern flanks, respectively, of the Amphitheater synform. The smaller Eureka, Rainy and Canwell MUM complexes are exposed north and northeast of the synform, along the southern flank of the Alaska Range itself; they have been cut and structurally stacked by south directed thrust faulting along the Broxson Gulch and related fault systems.

[17] The Fish Lake Complex [*Stout*, 1976] is a thick (1–1.5 km), extensive (>30 km), layered sill presumed to be comagmatic with the petrologically and geochemically similar, overlying Nikolai Greenstone lavas [*Ellis*, 2000]. It contains 4 ultramafic-to-mafic cycles of cumulate dunite, peridotite, pyroxenite and gabbro, and is the only known cyclically zoned, layered complex in Wrangellia. Exposures of the Tangle Complex are less extensive, and consist primarily of unlayered gabbroic and minor ultramafic sills of complex structural orientation. The Fish Lake and Tangle Complexes structurally and stratigraphically underlie pillowed and subareal basalt lavas of the Nikolai Greenstone in a west-northwest trending, gently west plunging synformal structure [*Stout*, 1976] that may have been a major feeder to the Nikolai magmatic system.

[18] Because the Amphitheater Mountains are well exposed and the basalts are relatively unmetamorphosed and undeformed compared to other exposures of the Nikolai LIP, this area provides a unique opportunity to study the plumbing of a large magmatic system. In addition, the area is of particular interest for mineral exploration because of its Ni, Cu, and platinum group element PGE) prospects, the largely unexplored ultramafic complexes, and its

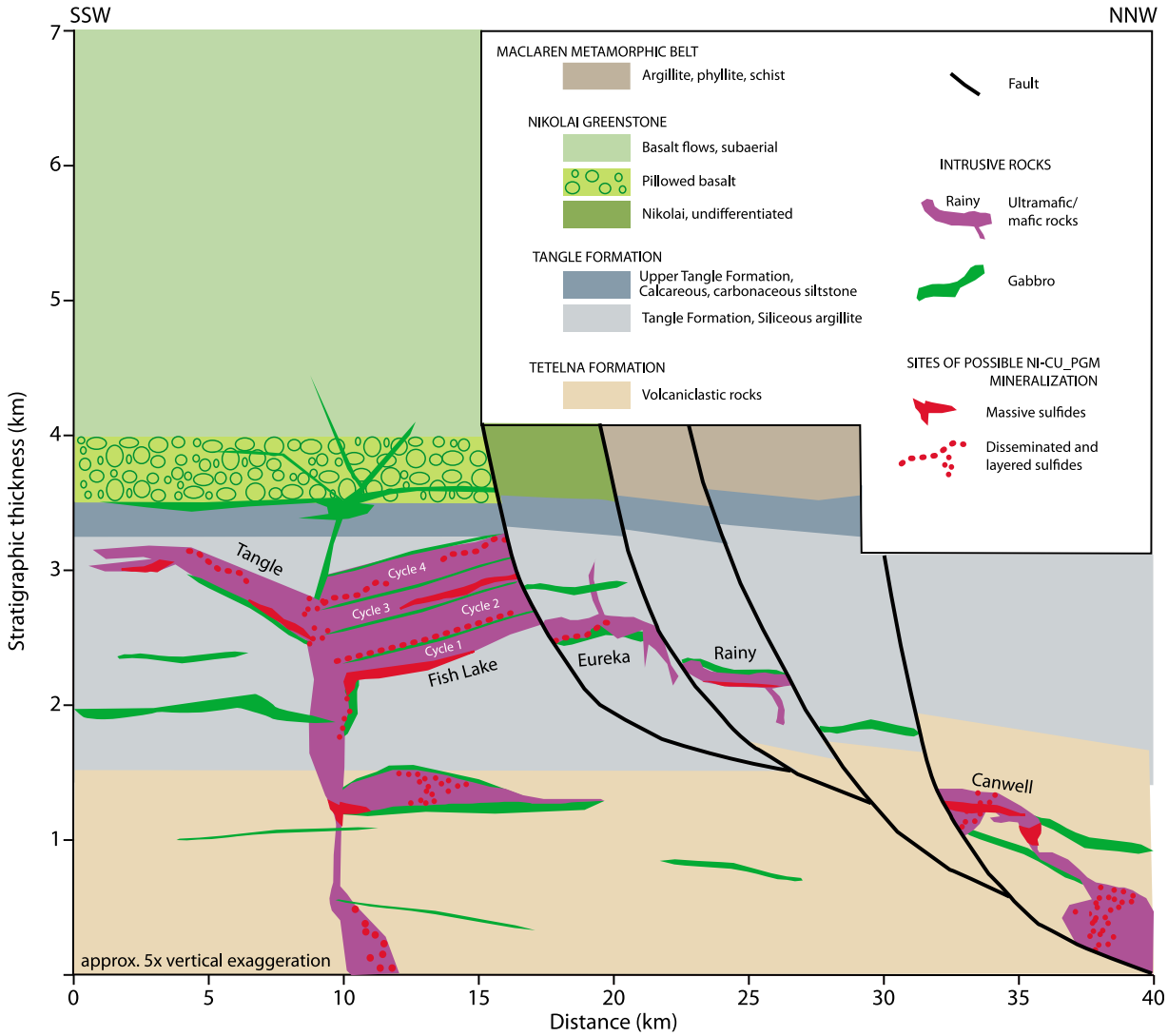

Figure 5. Schematic cross section showing a possible model for the structural relationships between mafic-ultramafic complexes within the Central Alaska Range belt. Aside from the Fish Lake and Tangle sills which coalesce at depth, it is unclear whether any of the other intrusive complexes were adjacent or connected during emplacement [after *Schmidt and Rogers*, 2007, Figure 11].

proximity to both the Denali and Richardson highways (Figures 1 and 2).

[19] One goal of this study is to differentiate between two hypotheses for development of the Amphitheater synform. A purely structural syncline, with stratigraphic and intrusive units folded long after deposition, would have different characteristics than a structure that formed synvolcanically (similar to a sag basin) due to subsidence as it filled with lavas and as the underlying magma chamber evacuated. Table 1 identifies characteristics that distinguish these two scenarios.

[20] 2-D and 3-D geophysical modeling should also resolve details (size, shape, and orientation) of the intrusions and their bounding structures. These models may therefore shed light on the geometry and possible connectivity between various Nikolai magmatic chambers (e.g., Rainy, Eureka, Fish Lake MUM complexes) at the time of basalt extrusion by clarifying the relative offset between stratigraphically different segments of the Nikolai LIP. Because many oceanic plateaus remain submerged and relatively inaccessible, little is known about their volcanic stratigraphy, their vent areas, or the intrusions that supplied them with magma. The Amphitheater Mountains, which expose both the Nikolai basalts and the MUM complexes of this large accreted oceanic plateau, offer a rare opportunity to investigate the plumbing system of a major oceanic LIP,

Table 1. Features Expected in Syncline Versus Structural Basin Settings for the Amphitheater Mountains Synform

Feature	Syncline	Synvolcanic Basin Related to Magmatic Emplacement
Flow thickness	Uniform across synform axis	Thicker toward center of synform
Flow orientation	Parallel from top to base of sequence	Steeper flows at base; shallower dip toward top
Total thickness of basalt	Uniform in all areas	Increases toward center of synform
MUM sill distribution	Random within sediments across region	Increase in number toward center of synform
MUM sill geometry	Variable across region	Increase in volume, thickness and continuity toward center of synform
Fish Lake/Tangle relations	Continuous sheet at same stratigraphic level; or no relationship	Connected but intruded at different stratigraphic horizons, or both thicken toward center of synform
Sub-Nikolai base	Sedimentary rocks ± sills below syncline	MUM magmatic root or keel below center of basin
Timing of formation	Late Cretaceous-Tertiary	Middle Triassic

and may provide information useful to the study of other LIPS such as the Proterozoic Midcontinent rift in the north central United States.

1.4. Mineral Resources

[21] Mafic LIPs worldwide host resources of platinum group elements (PGE), Ni, and Cu, the most economically significant of which are magmatic sulfide deposits in MUM intrusive complexes that supplied magma to the extrusive portions of the LIP.

[22] Mineral deposit types associated with the Nikolai LIP include (1) magmatic sulfide Ni-Cu, PGEs that are hosted in MUM intrusives, (2) basaltic copper deposits found in the Nikolai volcanics, and (3) Cu-Ag mineralization that occurs in the overlying sedimentary rocks. Disseminated to net-textured Ni-Cu sulfide mineralization with elevated values of PGEs has been identified in several Nikolai MUM intrusions in the study area. Massive sulfide deposits have not yet been identified, but are the primary target of current exploration activity. *Schmidt and Rogers* [2007] provide a detailed discussion of the metallogeny and mineral potential of the Wrangellia terrane in southern Alaska.

[23] The Nikolai LIP is similar geologically to the world class Noril'sk District in Russia (a layered intrusive feeder to the Permian Siberian Traps flood basalts) that has supplied abundant Ni and Cu from magmatic sulfide deposits. A genetic model for Noril'sk mineralization [*Naldrett et al.*, 1995, 1996], which ties Ni-Cu, PGE mineralization to the magma chemistry, magma flow dynamics, and magma plumbing of the layered MUM intrusions, has been applied to exploration in and near the Amphitheater structure [*Ellis*, 2000].

[24] Magmatic sulfide Ni-Cu-PGE deposits form by immiscibility between sulfide and silicate melts, with metals partitioning preferentially into the sulfide phase [*Naldrett and Lightfoot*, 1999]. The sulfide droplets typically collect in low-velocity areas within magma chambers and the plumbing systems that connect them. The volume and grade of mineralization is directly tied to the geometry and dynamics of the magmatic system, and the volume and flow rate of magma that passes through each part of the plumbing system. Besides velocity gradients and flow volume, the formation of magmatic sulfide mineralization also depends on sulfur availability from magma and wall rock, and the geochemical conditions (O, S fugacity) which favor immiscibility [*Naldrett and Lightfoot*, 1999].

[25] Because the geometry of the magmatic plumbing system is a critical factor controlling the distribution of sulfide minerals and PGE mineralization, defining the subsurface structure of the Nikolai vent system may help identify areas favorable for the accumulation of sulfide deposits.

2. Potential Field Methods

[26] Geophysical methods allow imaging of subsurface geologic bodies and structures and are particularly useful for regions that are poorly mapped and difficult to access. Variations in gravity and magnetic fields occur due to lateral contrasts in rock density and magnetic properties (magnetic susceptibility and remanent magnetization). Rock property contrasts may occur within a rock unit (e.g., lateral facies changes), across geologic structures (faults or folds), or at contacts with other rock units. The geometry and depth to sources, the character of the geomagnetic field, and the rock properties of sources all determine the character of a source's potential field anomaly. Despite the complexity and nonuniqueness of potential fields, gravity and magnetic data can be effectively used to resolve the geometry

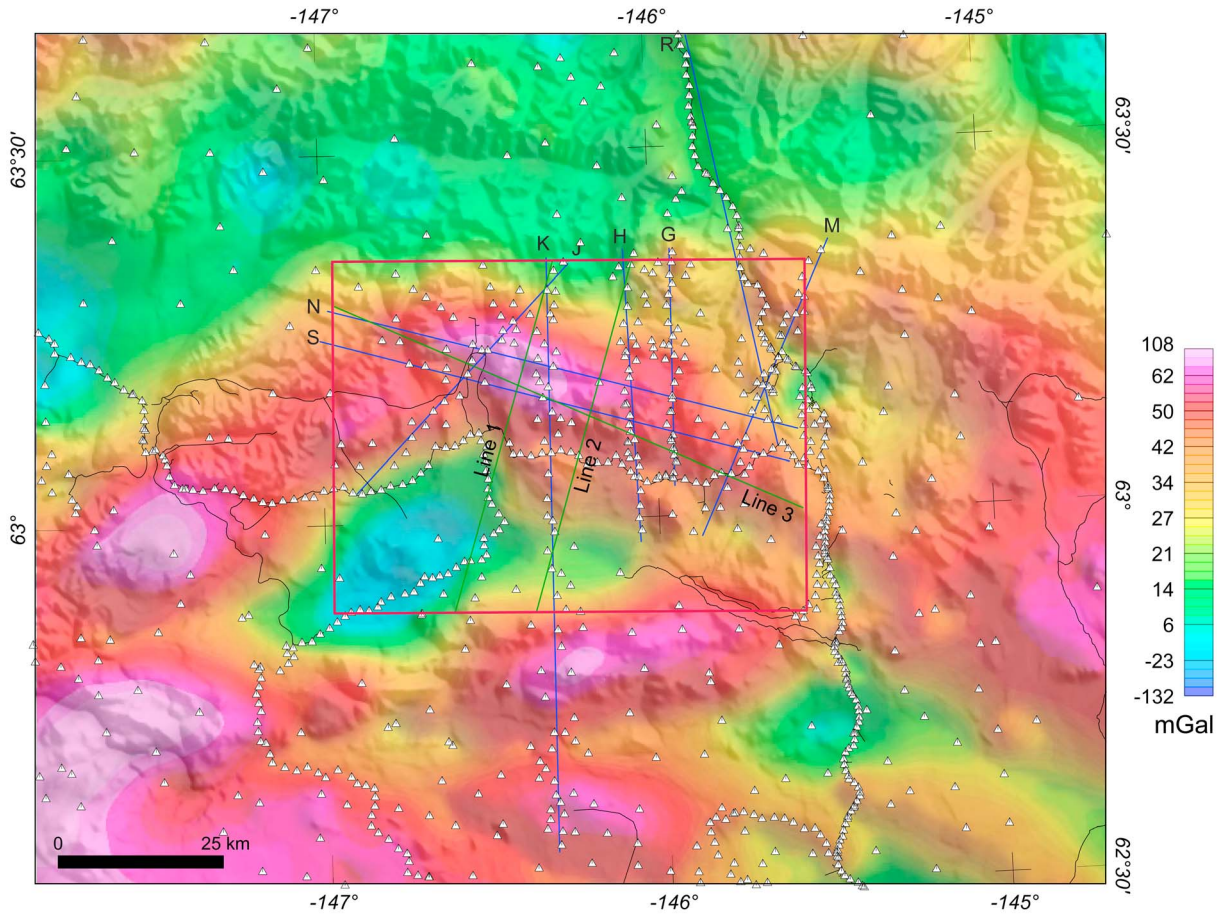

Figure 6. Regional isostatic gravity map centered on the Amphitheater Mountains. Triangles indicate the location of gravity stations. The 3-D model area is indicated by a red box. Profiles from the 2-D models are shown by blue lines. Green lines (lines 1–3) represent 2-D profiles extracted from the 3-D model.

and origin of sources, particularly when combined with other geologic constraints.

[27] Evaluating a region's potential for magmatic mineral deposits depends on understanding its intrusive history and how the deposit models of interest relate to the distribution of lithologic units and structures. Potential field methods are useful in exploration for magmatic mineral resources because the ore minerals of interest (e.g., chalcopyrite, pyrrhotite) are dense and/or magnetic and because they successfully map dense and often magnetic mafic and ultramafic igneous rocks that host the deposits.

[28] In the Amphitheater Mountains area, the physical properties of mafic volcanic rocks and ultramafic sills of the Nikolai magmatic system contrast strongly with the surrounding metasedimentary rocks to produce prominent gravity and magnetic anomalies [*Glen et al.*, 2007a]. At some Ni-Cu prospects in the Rainy complex, net-textured and disseminated sulfides occur with magnetite-bearing dunite which produces coincident gravity and magnetic anomalies.

[29] Because detailed potential field data are available for the study area, the Amphitheater Mountains provide a unique opportunity to integrate geologic and geophysical methods to understand the structure and character of a major vent to the Nikolai LIP and its influence on metallogeny.

[30] Magnetic data were compiled from three regional aeromagnetic surveys (AK08, Delta River, and survey 193; Figure 7). Gravity and magnetic profiles for modeling were derived from 250 m grids generated from these data.

2.1. Gravity

[31] Over 175 new gravity stations were collected along several profiles (Figure 6) through the Amphitheater Mountains study area and, combined with existing regional data [*Morin and Glen*, 2002, 2003], provide roughly 2 km station spacing along the

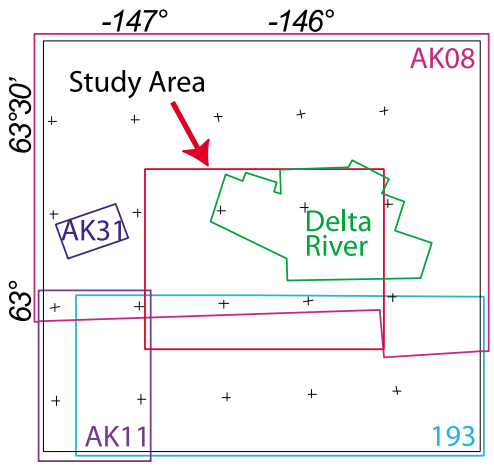

Figure 7. Index map of the boundaries of aeromagnetic surveys covering the Amphitheater Mountains study area. Red outline indicates the 3-D model area. Individual surveys are denoted by colored polygons and labels. Survey boundaries outside the margin (black outline) are schematic and indicate only the general direction in which the surveys extend.

profiles. An isostatic gravity map of the study area (Figure 6), derived from the data described above, reflects anomalies produced by contrasts in crustal density, with long-wavelength anomalies with smooth gradients originating from sources at depths greater than those of short-wavelength anomalies with steep gradients. To obtain data reflecting lateral variations in crustal density, raw gravity measurements were reduced using standard methods [*Dobrin and Savit*, 1988; *Blakely*, 1995] to remove the effects of elevation, topography, and the total mass, rotation, and ellipsoidal shape of the Earth, yielding the complete Bouguer gravity anomaly (CBA). Although the CBA reveals lateral density variations at short-wavelength scales, it does an inferior job isolating longer wavelength features, because these are often masked by broad anomalies due to crustal roots that isostatically compensate topographic loads. The isostatic correction attempts to correct for the effects of these compensating masses. Although there is some indication that the southern Alaska margin is out of isostatic balance due to effects of the subducting pacific plate [*Barnes*, 1976; *Saltus et al.*, 2007], use of the isostatic anomaly in our modeling is considered to have little if any effect on our modeling results and conclusions, given that the extent of the study area is small compared to the wavelength of the isostatic imbalance.

2.2. Magnetics

[32] The magnetic map (Figures 7 and 8) for the model area was compiled from three surveys: AK08 flown at 1000′ above ground level (AGL) along north-south lines 3/4 mile apart [*Connard et al.*, 1999]; Delta River, flown 200 feet AGL along northwest and northeast oriented lines 1/8 and 1/4 mile apart [*Burns*, 2003], and survey 193, flown at 4000′ barometric elevation along north-south lines 1 and 2 miles apart. Survey 193, which covers only the southernmost study area, was derived from a grid of digitized contours of the original survey maps [*Andreasen et al.*, 1958; *Saltus and Simmons*, 1997].

[33] The magnetic map reveals variations in the magnetic field that arise from contrasting magnetic properties of rocks, such as variations in remanent magnetization or the amount and type of magnetic minerals. The shallower the depth of a body, the higher the amplitude, the shorter the wavelength, and the sharper the gradients of its magnetic anomaly.

[34] Although crustal fields depend on both induced and remanent crustal magnetization, remanence is often ignored because in many cases its magnitude is negligible or because its direction lies close to the induced field direction. Remanence however, may have a significant effect, particularly in the case of strongly magnetic units such as mafic and ultramafic rocks like the Nikolai Greenstone and associated intrusions.

[35] Uncertainties in the magnetic response also arise from deviations of the instrument-bearing aircraft from the designated draped or fixed elevation. This uncertainty particularly effects the interpretation of older surveys for which aircraft elevation data are not available. The uncertainty is most significant in steep or highly variable terrain where the deviations in elevation are likely to be the greatest.

2.3. Rock Properties

[36] Because gravity and magnetic field anomalies reflect variations in the density and magnetic susceptibility of the underlying bedrock, these rock properties are essential components to potential field modeling. To aid modeling of the potential field data, magnetic susceptibility (>700 measurements) and density measurements (>300 samples) were made on rock samples from the area, and combined with rock data from previous surveys in south central Alaska. For details on gravity, magnetic, and rock property data, refer to *Glen et al.* [2007a, 2007b], *Morin and Glen* [2002, 2003], and *Sanger and Glen* [2003]. In general, average grain density of rocks in the region increases from sedimentary, and felsic- to intermediate-igneous rocks, to mafic igneous and

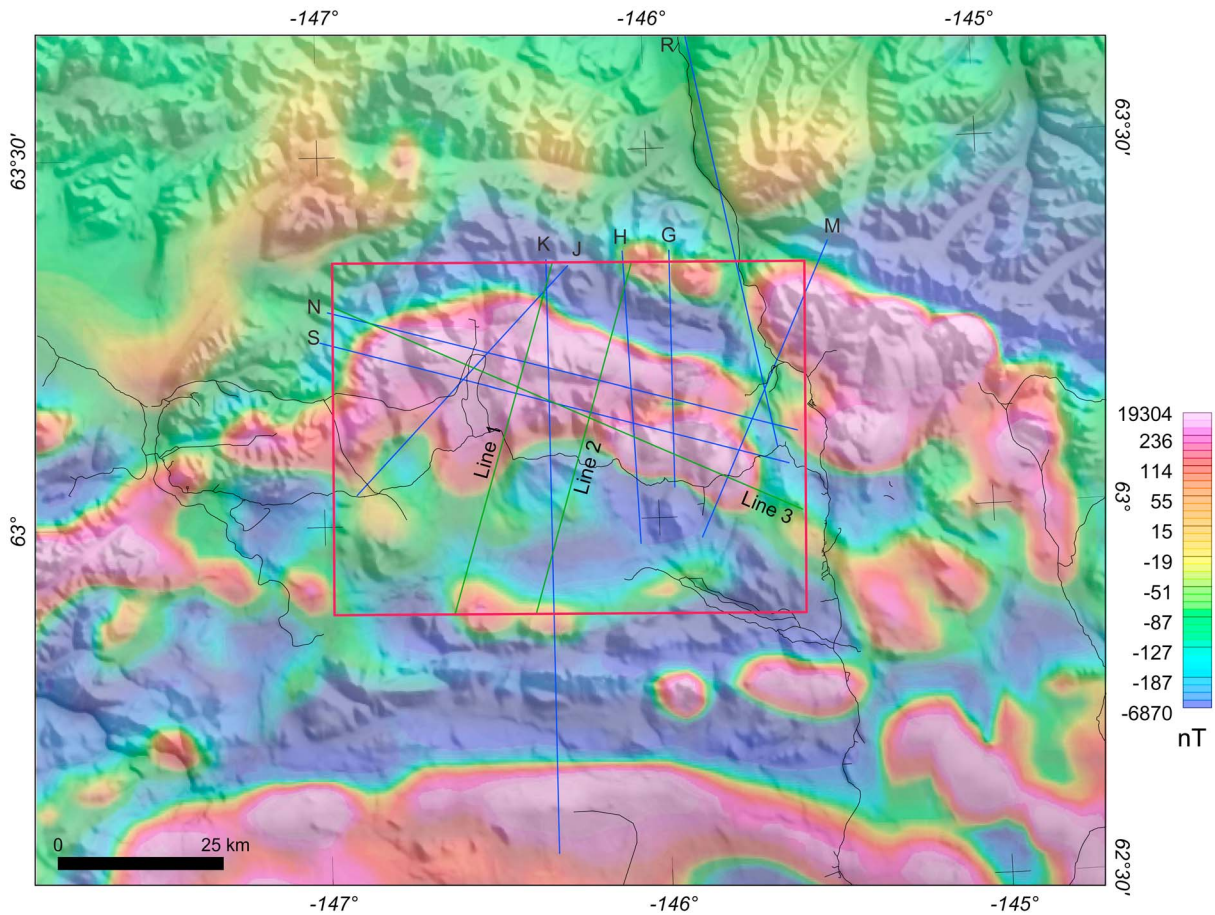

Figure 8. Regional residual magnetic anomaly map centered on the Amphitheater Mountains. The 3-D model area is indicated by a red box. Profiles from the 2-D models are shown by blue lines. Green lines (lines 1–3) represent 2-D profiles extracted from the 3-D model.

metamorphic rocks, consistent with general trends [*Olhoeft and Johnson*, 1989]. Magnetic susceptibilities (measured from outcrop and hand sample) are low for sedimentary and felsic intrusive rocks; moderate for metamorphic and intermediate igneous rocks; and highest for mafic and ultramafic igneous rocks that generally contain more abundant strongly magnetic minerals (note that the magnetization of a rock depends primarily on its content of magnetic minerals such as magnetite [*Carmichael*, 1982]). Magnetic remanence can also be an important factor in controlling magnetic anomalies, particularly in strongly magnetic volcanic rocks. For many potential field studies, magnetic remanence data is not available. Fortunately though, remanence is often either negligible, due to a much stronger induced component that is controlled by the magnetic susceptibility, or dominated by a present field overprint magnetization that can be considered equivalent to an induced component of magnetization. In our study we make use of previously published remanence data for the Nikolai Greenstone. Rock properties assigned to the model presented here (Table 2) are based on a combination of samples and outcrop measurements taken from the study area, and data derived for similar lithologies obtained from an national database (D. Ponce, USGS, unpublished data, 2010) consisting of over 17,000 measurements.

3. Geophysical Maps

[37] Gravity and magnetic highs in south central Alaska (Figures 6 and 8) reflect mafic and ultramafic rocks associated with the Nikolai Greenstone [*Glen et al.*, 2007a]. Gravity high G1 (Figure 9a), centered on the axis of the Amphitheater synform, reflects dense Nikolai Greenstone and associated ultramafic intrusive rocks in the shallow to middle crust. A less pronounced high occurs over the Canwell ultramafic complex (feature G6, Figure 9a).

Table 2. Rock Properties of Density, Magnetic Susceptibility, and Magnetic Remanence Assigned to Layers of the 3-D Model[a]

		Density (g/cm^3)			Magnetic Susceptibility (cgs 10^{-6})			Magnetic Remanence		
Layer	Unit	Min	Max	Density	Min	Max	Susc	Mag (emu/cm^3 × 10^{-6})	Inc (deg)	Dec (deg)
1	Maclaren	2.74	2.79	variable			20			
2	Canwell	2.78	2.84	variable			6800			
3	Rainy			2.77			1000			
4	North mix	2.77	2.80	variable			1000			
5	Nikolai			2.82			3000	1000	−26.7	98.5
6	Tangle and sills	2.68	2.83	variable	0	9360	variable			
7	UMs			2.83			9400			
8	Gulkana MUMs			2.82			1000			
9	Gulkana			2.74			150			
10	South mix	2.77	2.78	variable	350	2520	variable			
11	basal layer			2.8			9000			

[a]Max, maximum; min, minimum; Susc, magnetic susceptibility; Mag, magnetization; Inc, inclination; Dec, declination.

[38] Similarly, magnetic highs M1, M2, M6 and M7 (Figure 9b) result from the Fish Lake, Tangle, Rainy, and Canwell MUM complexes, respectively.

[39] Gravity and magnetic contrasts from north (G7, M10) to south (e.g., G3 and G4, M5) across the margins of the Amphitheater structure, reflect weakly magnetic, low-density metasedimentary rocks in contact with dense, magnetic rocks of the Nikolai system. Gravity high G2 and the corresponding moderate magnetic anomaly (M11) are located over Nikolai basalts whose basement is poorly known.

[40] Magnetic high M6 (Figure 9b), which corresponds with anomaly 17 of *Campbell and Nokleberg* [1997], is inferred to result from the Rainy intrusive complex. Gravity high G5 is the northern edge of a very large high over the Alphabet hills (Keg high of *Glen et al.* [2007a]) and corresponds in part with an elongate magnetic low south of the study area (south of feature M4). Prominent gravity lows (G3 and G4, Figure 9a) coincident with a regional magnetic low (M5) reflect weakly magnetic, low-density sedimentary rocks, probably Tertiary basin fill.

[41] A narrow E-W trending magnetic high (M4, Figure 9b), corresponds in part with the "Maclaren-Gulkana anomalies" of *Andreasen et al.* [1964], and with the "Media high" of *Campbell and Nokleberg* [1986], along the edge of gravity high G5. The M4 anomaly, although partially covered by Quaternary sediments reflects the presence of Jurassic(?) ultramafic rocks.

[42] A moderate magnetic anomaly (M8) at the southeast edge of the study area corresponds with part of "Excelsior Creek anomalies" of *Andreasen et al.* [1964] and is associated with a moderate gravity high. The source although largely concealed, may reflect mafic volcanic rocks which outcrop nearby.

4. Two-Dimensional Models

[43] Two-dimensional potential field models were constructed along eight geologically selected profiles (locations shown in Figure 2a) through the study area. These eight 2-D models were used as the initial input to build the 3-D model presented here (see Figure 10 for an example of one of these 2-D profile models). Model magnetic fields were calculated on a datum that drapes topography at a nominal height of 1000 feet (305 m), which reflects the elevation of the merged data compilation used [*Saltus and Simmons*, 1997].

[44] The 2-D profiles (1) include the highest density of gravity data, (2) coincide with geologic cross sections, and (3) are roughly perpendicular to the strike of geologic units (Figures 2 and 6). They were constructed using GMSYS, a forward modeling program that allows for nonorthogonal model strikes. Sources were approximated by blocks that varied in the ± Y directions (commonly referred to as 2 3/4-D modeling). Forward modeling of this type [*Talwani et al.*, 1959; *Blakely and Connard*, 1989] can critically constrain viable structural models when combined with geologic (bedrock, drilling) and other geophysical data (magnetotelluric, seismic, etc.). Nonetheless, potential field forward models are critically dependent on the modeling assumptions inherent in the simplification of complex geology by simple geometric block models.

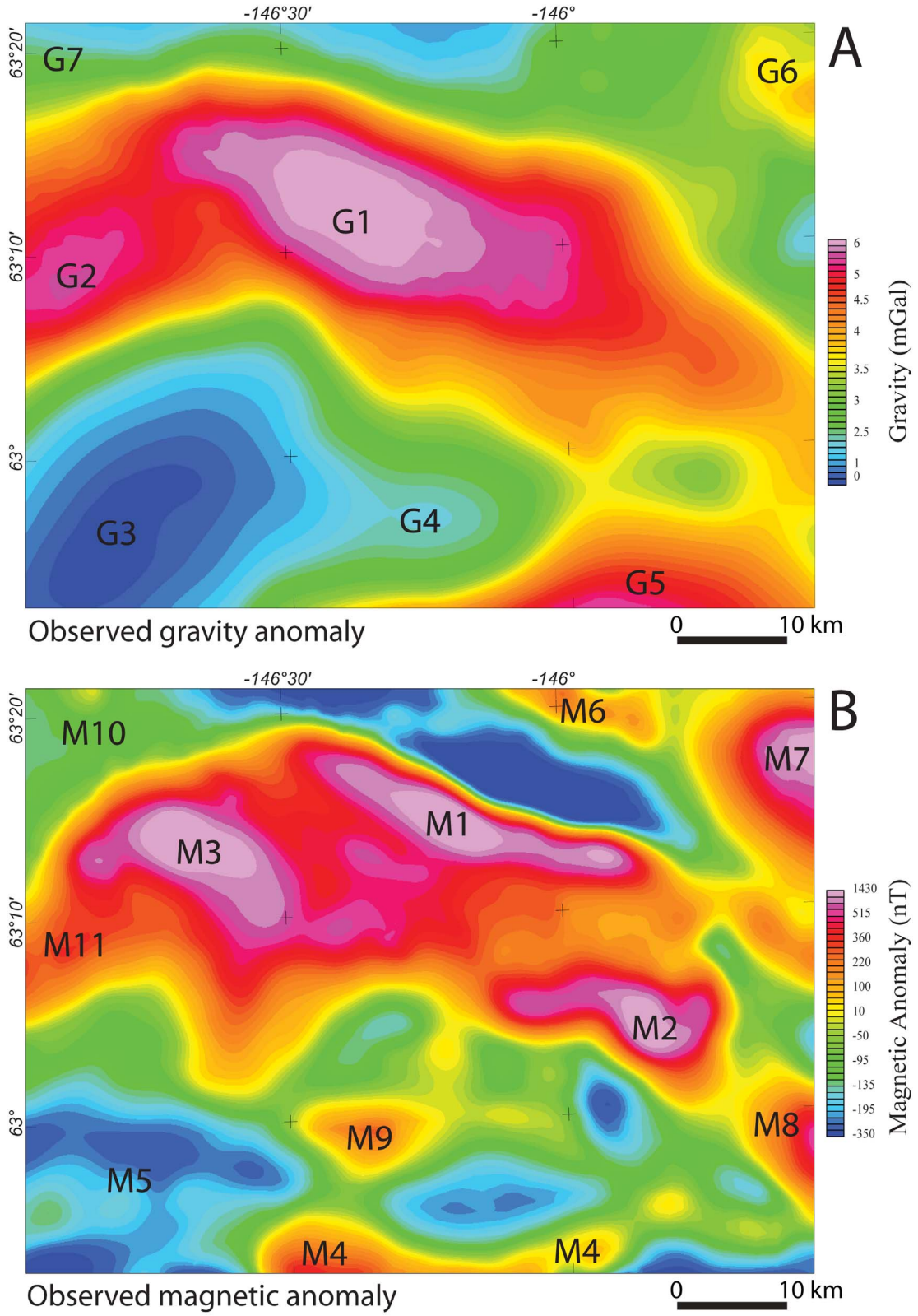

Figure 9. (a) Isostatic gravity map of the Amphitheater 3-D model area. (b) Residual magnetic anomaly map of the Amphitheater 3-D model area. Labeled anomalies are discussed in the text.

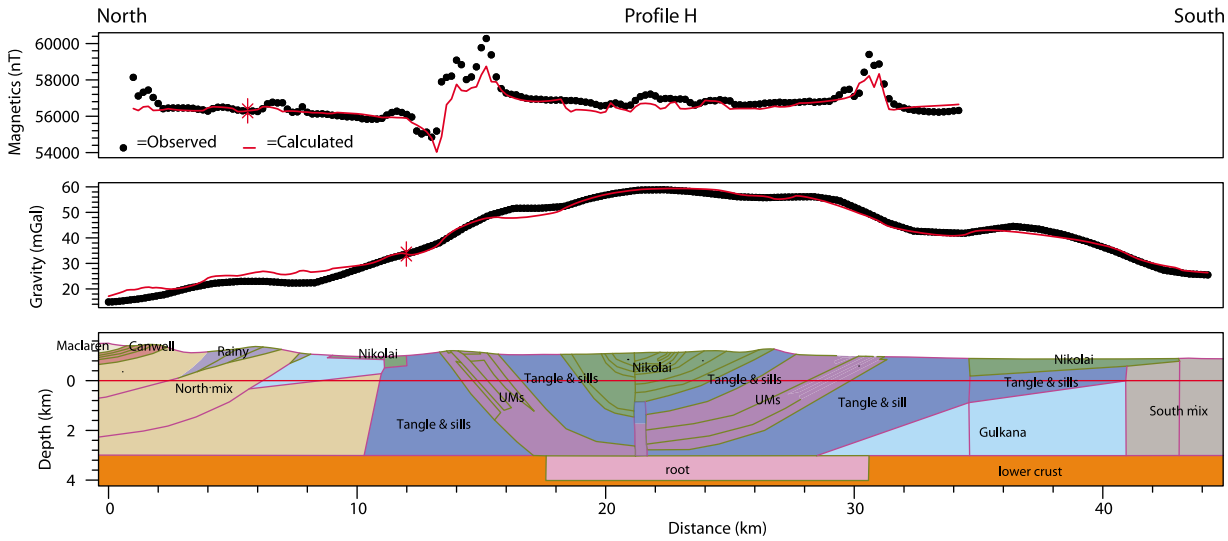

Figure 10. Two-dimensional potential field model along profile H (see Figure 2a for profile location). (top and middle) Observed (black circles) and model (red line) anomalies for magnetic and gravity fields, respectively. (bottom) The potential field model with individual model bodies colored by rock unit.

[45] Our 2-D model bodies consisted of horizontal tabular prisms or blocks with long axes parallel to the regional strike of bedding. Their surface extents were constrained to be consistent in size, shape and orientation with mapped geologic units. The subsurface geometries of the model bodies were determined through a forward method to match calculated anomalies with observed anomalies within the limits imposed by surface geology, rock property data, and maximum horizontal gradients (MHG). The MHG, best expressed over bodies with near vertical boundaries [*Grauch and Cordell*, 1987; *Cordell and McCafferty*, 1989], reflect abrupt lateral changes in density or magnetization, and are useful for estimating the horizontal extent of buried sources. *Glen et al.* [2007a] discuss the details of these methods and provide maps and interpretations of regional-to-local scale geophysical domains that span the study area.

[46] Density and magnetic properties of 2-D bodies were adjusted iteratively to match observed gravity and magnetic profiles while staying within the limits of values (1) derived from the corresponding geologic units [*Sanger and Glen*, 2003] or (2) from values derived from similar lithology (based on an unpublished database of western U.S. rock properties (D. Ponce, USGS, 2010)). Magnetizations were assumed to parallel the present field direction, (56,500 nT, 75.5° inclination, and 27° declination). An exception was made for Nikolai basalts to which a remanent magnetization [*Hillhouse and Gromme*, 1984] was assigned, in addition to the induced component.

[47] Although potential field models are relatively effective at constraining the depth to the top of an anomaly's source, or the location and dip of its edges, they are relatively insensitive to the depth of a source's base and therefore characterize the shallow and deeper crust with different degrees of detail. Because of the inherently 3-D structure of the plunging Amphitheater synform, 3-D modeling was required to adequately characterize the geometry of the structure and surrounding features.

5. Three-Dimensional Model

[48] To construct the 3-D potential field model, we first exported surfaces defined as the top or bottom surfaces of layers from our 2-D profile models (e.g., profile H, Figure 10). This required simplifying the geology to include a total of eight layers. As a result, some features in the 2-D models are not represented in the 3-D model, including layers that bound the Eureka Complex, or the cyclic layering within the Fish Lake sill. In addition, Quaternary units (including alluvial (Qa), fluvial-lacustrine (Qfl) and undivided Qu), Tertiary volcanic rocks, Tertiary sediments, and various Cretaceous to Tertiary granites across the map were not distinguished in our simplified layers.

[49] The exported 2-D surfaces, together with outcrop constraints (Figure 11), were gridded, within a

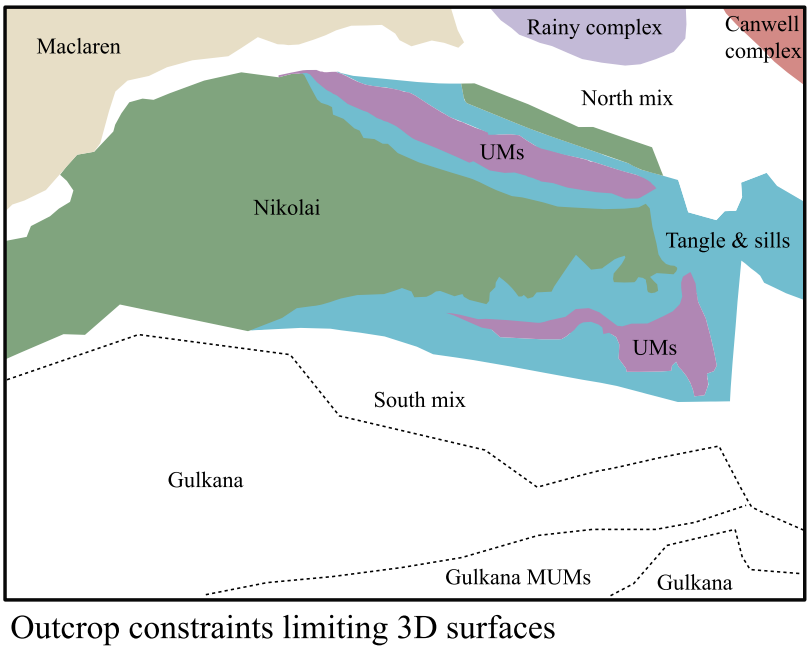

Figure 11. Map of outcrop constraints used in the initial construction of the 3-D model.

model area of 50 × 70 km, to produce a set of eight grid layers from which the 3-D model was initially constructed. Additional layers (Figure 12 were added to account for features not crossed by the 2-D profiles. Once all the layers were in place, the 3-D model was then modified through a series of forward and inverse steps to minimize the error between observed and calculated anomalies (Figure 13). The final model consists of 11 surfaces, including topography and a basal surface at 3 km depth (Figure 12) representing regional crustal basement.

[50] A list of the model layers and the geologic units they represent is given in Table 2. In the model, each surface (layer) represents the top of a particular unit. These include (from top to bottom in model order): Maclaren (equivalent to the topographic surface), Canwell, Rainy, North mix, Nikolai, Tangle and sills, UMs, Gulkana MUMs, Gulkana, South mix, and the basal layer. Herein, we will refer interchangeably to units and the model layers that represent their tops. We note that this order was imposed largely for modeling convenience and does not imply the actual stratigraphic order of units.

[51] The Maclaren layer includes the granites (TKg) in the northwest portion of the study area (Figure 2b), plus metasedimentary rocks (Jrarg, Jrph, and Jrsch) and a small piece of Clearwater terrane (unlabelled unit in the westernmost part of map). Rainy and Canwell ultramafic rocks are grouped (along with Eureka, Fish Lake and Tangle ultramafics) as the

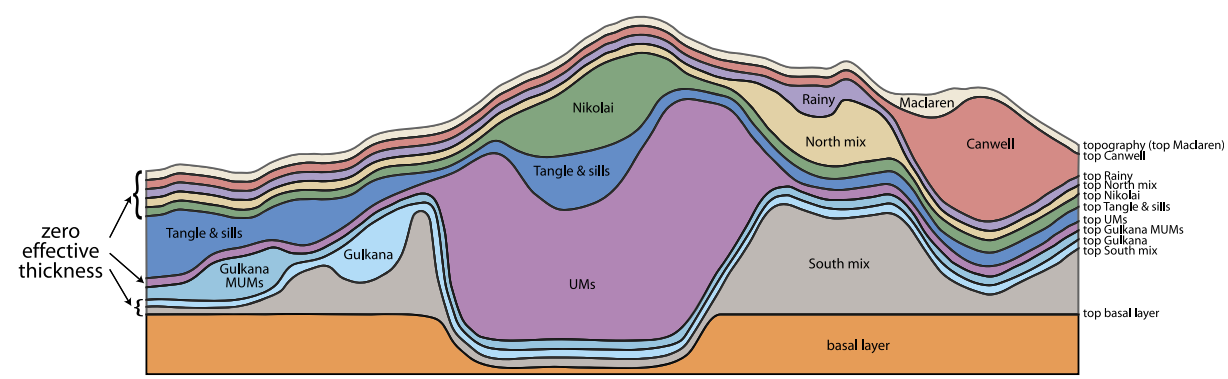

Figure 12. Schematic of model grid layers.

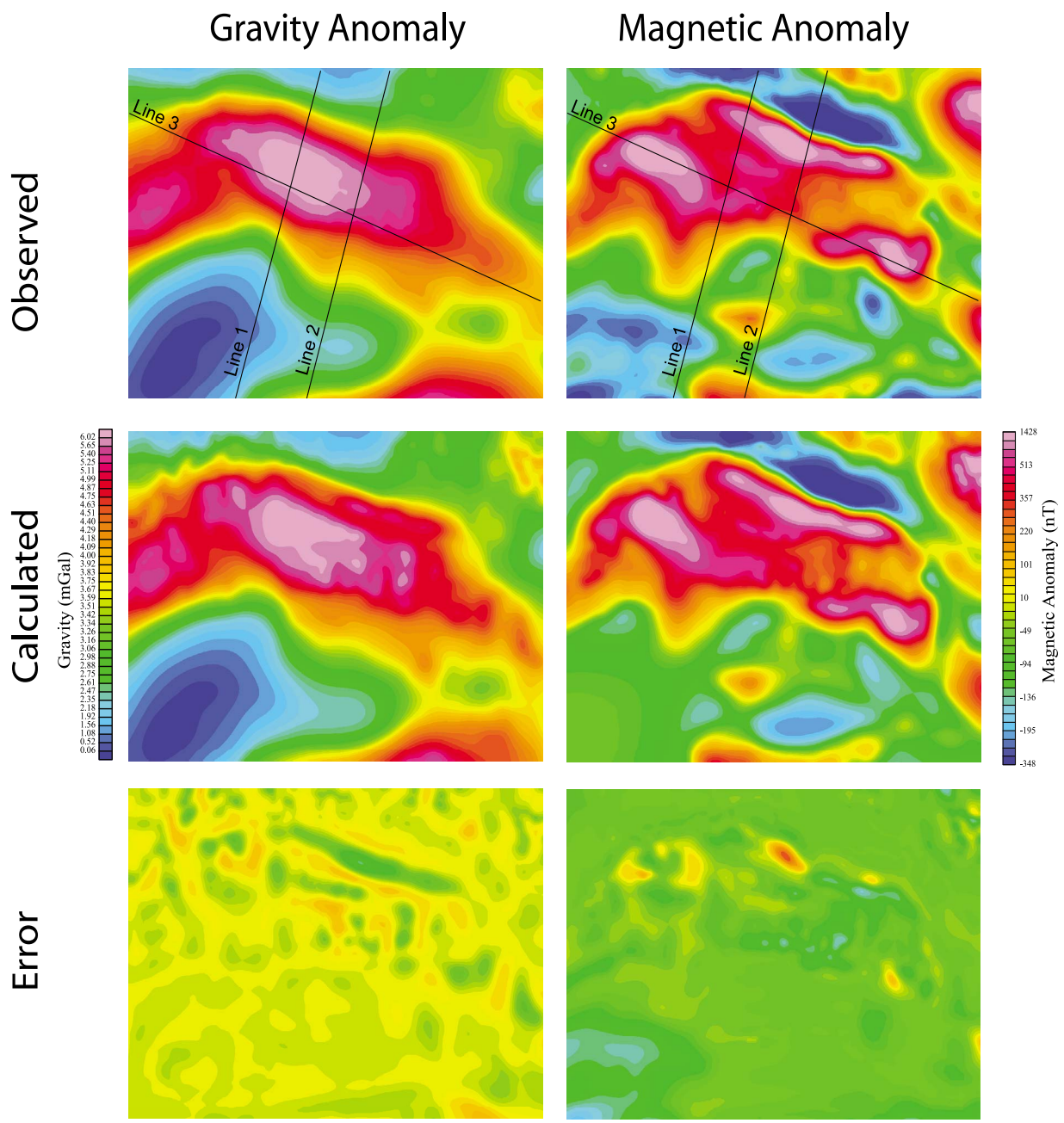

Figure 13. Observed, calculated, and misfit maps of gravity and magnetic fields for the Amphitheater study area. Calculated maps are generated from the 3-D model. Misfit maps reflect the difference (error) between observed and calculated maps. Black lines (lines 1–3) show the locations of 2-D model profiles extracted from the 3-D model.

same lithologic unit (Trum) on the geologic map (Figure 2b), but are represented by unique 3-D model layers. The North mix model layer includes volcaniclastics and sediments (PlPu) older than the Tangle Formation, together with Tertiary sediments (Ts), Eureka ultramafic rocks, and small outcrops of Nikolai (TrNu) that occur north of the Amphitheater synform proper. The Nikolai, Tangle and sills, and ultramafic layers form the core of the synform. The Gulkana MUMs layer represents geophysically distinct gabbro and ultramafic rocks within the Gulkana metamorphic complex. The Gulkana layer includes the remaining metaintrusive and metasedimentary rocks of the Gulkana metamorphic complex (Jrmet). The South Mix layer includes Nikolai Greenstone outside the synform, some lower Tangle Formation,

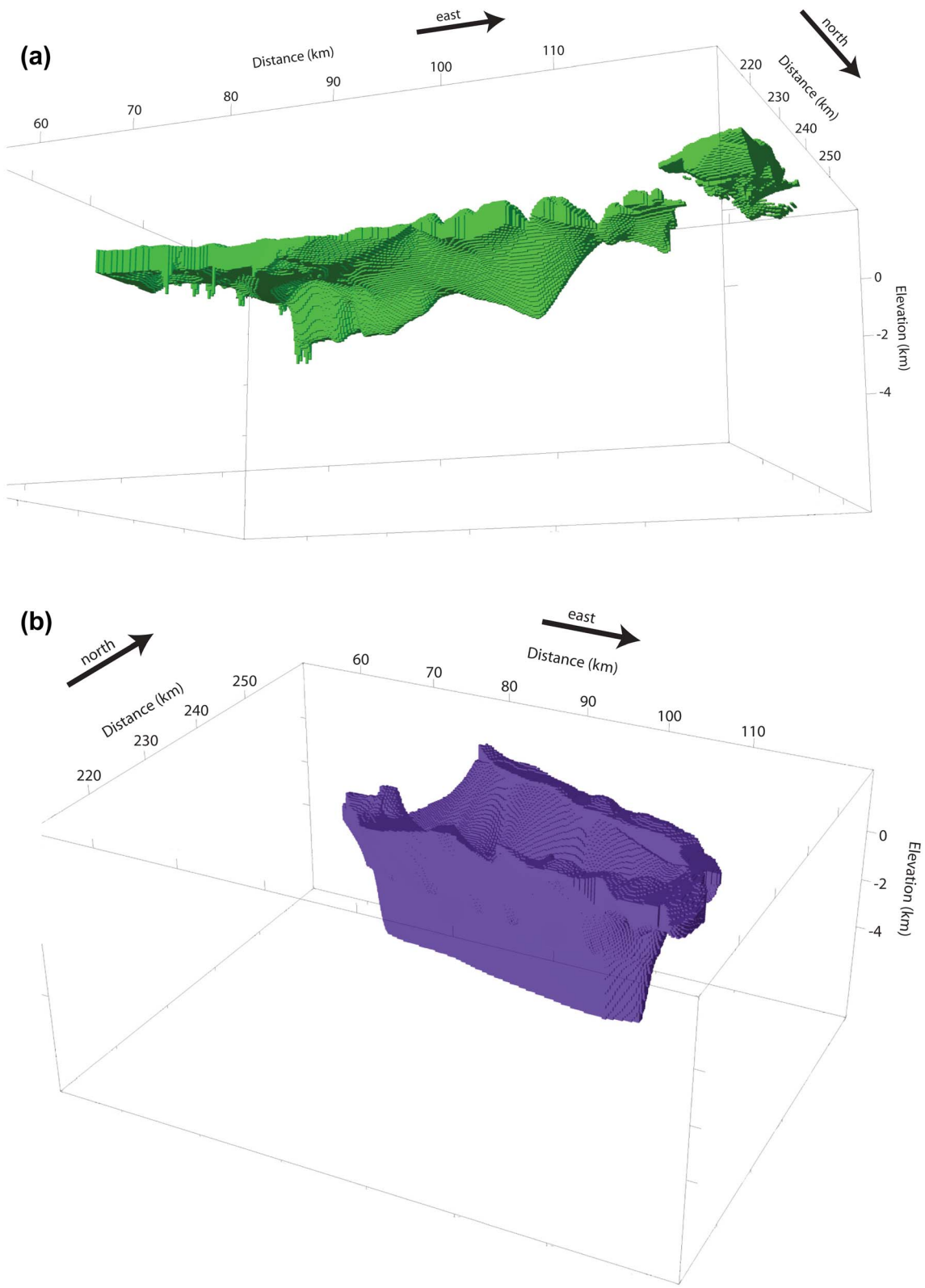

Figure 14. Oblique 3-D views of the (a) Nikolai Greenstone (viewed from below, looking toward NW) and (b) ultramafics (viewed from the SE, looking toward NW).

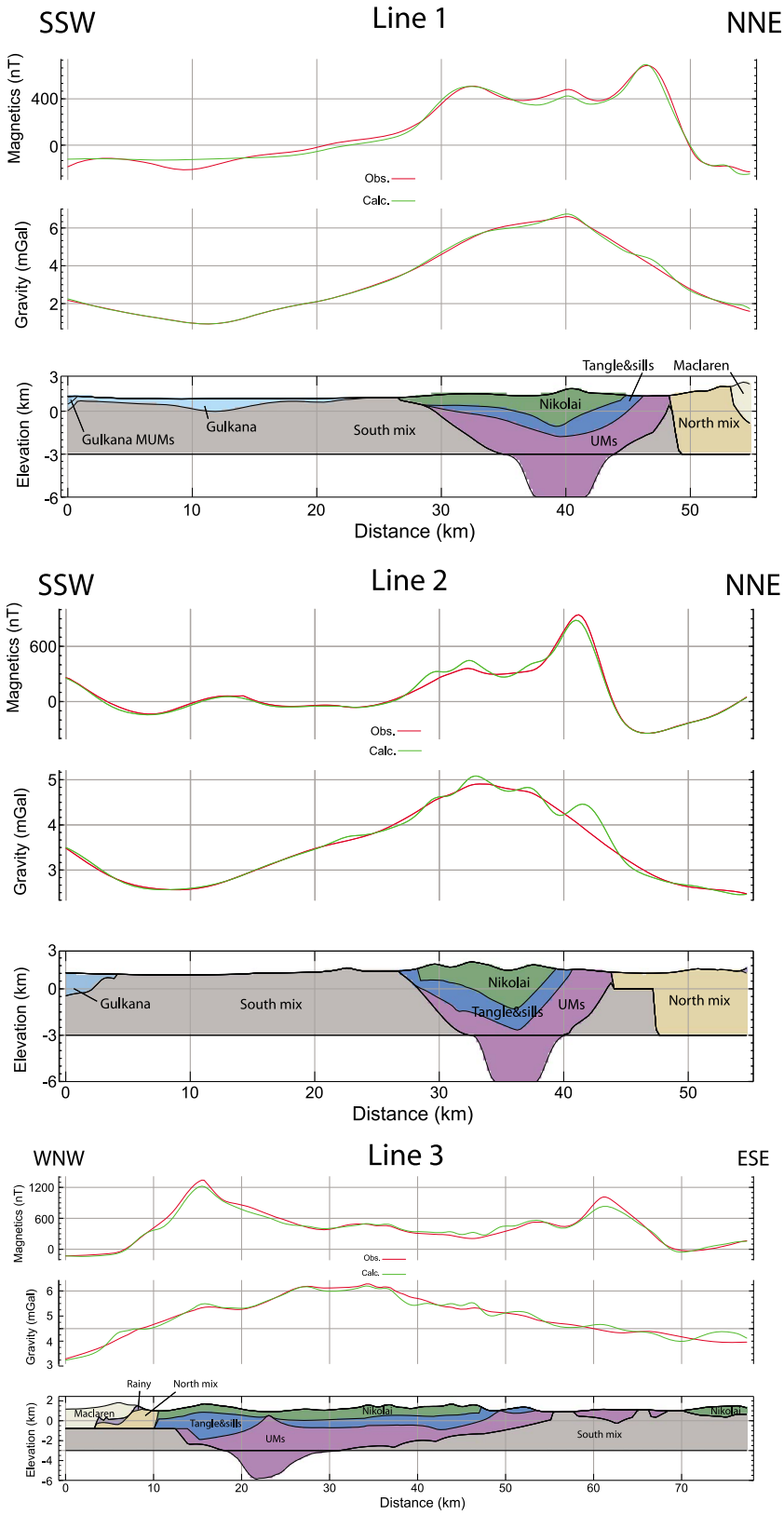

Figure 15. Two-dimensional profiles of the 3-D potential field model (see Figures 2a, 6 and 8 for profile locations) for lines 1, 2, and 3.

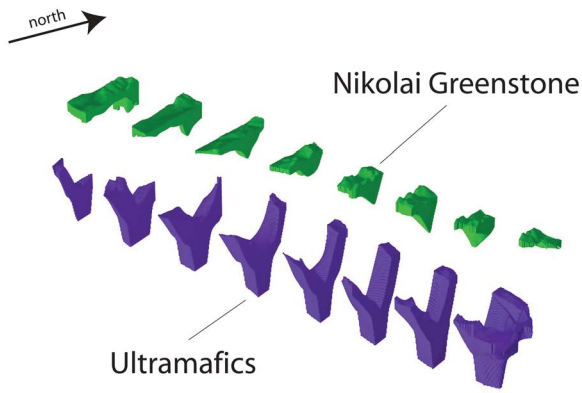

Figure 16. Cutaway slices of the 3-D model layers of Nikolai and ultramafics. Slices (excluding the two ends) are 5 km thick. Nikolai and ultramafic layers have been offset vertically from each other.

minor Tertiary volcanic and granitic rocks, and metahornblende andesite that is probably low-grade meta-Nikolai (mha).

[52] The 3-D model, like the 2-D models from which it was derived, is more sensitive to shallow crustal sources. As a result, most of the complexity in the model occurs in the shallow-level crust with only the deepest, ultramafic portions of the Amphitheater synform extending to depths below 3 km. For the 2-D models, the transition between shallow and mid-crustal levels was based on a regional common depth to the top of matched-filtered layers of gravity and magnetic data (at 2.5 and 3.3 km, respectively), that suggest a change in crustal character at that depth [*Glen et al.*, 2007a, 2007b].

[53] The largest misfits in gravity and magnetics remain over the northern edge of the synform over outcrops of ultramafic rocks of the Fish Lake Complex. This may result from an unaccounted for component of remanent magnetization in the intrusive units of the complex. To illustrate the geometry and fit of the 3-D model we show 3-D views of the Nikolai and ultramafic layers (Figure 14) as well as several 2-D cross sections (Figure 15) and cutaway slices (Figure 16) taken from the 3-D model (see Figures 2a, 6, and 8 for location of profile lines 1–3).

[54] The regional structure is complicated by Cretaceous(?) to Recent thrust, strike-slip, and tear faults related in part to the Denali Fault Zone. Furthermore, the facies architecture of sedimentary and volcaniclastic rocks into which the magmatic system was emplaced is very poorly understood. Despite this, the model demonstrates that the Amphitheater structure forms a relatively simple, coherent synform, gradually thickening and plunging westward, and extending to depths below 5 km, suggesting that the magmatic feeder system to the Nikolai LIP is larger and more extensive than previously known. We note that the model is least sensitive to the deepest extents of the structure, making it difficult to distinguish whether the ultramafic rocks deepen into a narrow, multikilometer keel similar to the Muskox intrusion in the Northwest Territories, Canada [*Irvine*, 1980], or diminish at depth. Nonetheless, our model requires a significant volume of ultramafic material at depth, which forms a funnel-like structure that we interpret as the upper portion of a chamber that supplied magma to the Nikolai lavas and fed emplacement of the largest Nikolai-related magmatic intrusions. Volume calculations on the model layers indicate the Amphitheater synform contains approximately 2000 km^3 of ultramafic rocks and over 900 km^3 of Nikolai basalts.

6. Discussion

6.1. The 3-D Model

[55] The Amphitheater Mountains, which contain cyclically layered and differentiated ultramafic intrusives that fed the overlying Nikolai lavas, is the only known vent for the Nikolai LIP. Even if other vents fed some portions of the volcanic province, the Amphitheater structure must be a major eruptive center as the stratigraphic thickness of Nikolai here is at least equal to that at the type section in the Wrangell Mountains. Despite the exceptional exposures of the Amphitheater structure, the vast majority of the mafic and ultramafic rocks in the complex reside in the subsurface. Three-dimensional potential field modeling offers the opportunity to characterize the extent of subsurface units, and allows for volume calculations of potentially mineral resource-bearing units like the Nikolai and associated ultramafic intrusions. The model reveals the presence of a significant, westward plunging subsurface ultramafic material below the Amphitheater Mountains, substantially expanding the mineral potential of the complex (see animations S1–S3 in the auxiliary material).[1] Irregularities in the generally smooth surfaces of the ultramafic intrusions may indicate areas of magmatic/hydraulic complexity or quiescence conducive to segregation or accumulation of sulfide minerals. Estimated volumes of Nikolai basaltic and related ultramafic rocks, based on the 3-D model are on the order of 1000 and

[1]Auxiliary materials are available in the HTML. doi:10.1029/2011GC003508.

2000 km^3, respectively. Details of the model may help to distinguish between the two end-member models hypothesized for the origin of the Amphitheater structure (Table 1).

6.2. Syncline Versus Sag Basin Models

[56] One of the goals of this work was to define the crustal structure below the Amphitheater Mountains, in order to determine whether the units exposed represent a syncline (a postdepositional fold due to regional deformation, in which the core preserves the stratigraphically youngest rocks) as previously mapped, or a sag basin that represents a structural downwarp or extensional basin formed during emplacement of the Nikolai basalts. The latter could form structurally, with basin-bounding faults also acting as a conduit for magma eruption, or by deflation as a magma chamber at middle to shallow crustal levels was emptied, and collapsed under the weight of the overlying basalts.

[57] Geologic observations favor a synvolcanic basin (Table 1) that developed during emplacement of the Nikolai Greenstone. Basalt flows thicken toward the center of the synform and dips shallow upward [*Nokleberg et al.*, 1992; *Greene et al.*, 2010]. In addition the lack of small-scale folding in the Tangle Formation sediments (B. Ellis, oral communication, 2005) suggests the synform is not a product of postdepositional folding.

[58] Certain features of the geophysical model also support the hypothesis that the Amphitheater structure developed primarily as a sag basin. Density and magnetic gradients within the Tangle sediments suggest that volume of gabbroic sills varies substantially with a general increase toward the center of the synform. Although they coalesce at depth, the Fish Lake and Tangle sills do not occur at the same stratigraphic level below the Nikolai, making it unlikely that they were once a single planar intrusion folded by regional deformation. A deep (>3 km) root of dense material along the axis of the sag basin plunges westward along with overlying stratigraphic contacts, but the model suggests asymmetry with more of the root along the southern (Tangle) side. Asymmetry of the sag basin is also suggested by a central structure (synvolcanic fault?) parallel to 7 Mile lake, which divides and offsets two separately dipping limbs of Nikolai basalts. This central axial structure overlies the dense ultramafic root and may have been the primary magma conduit for the mafic-ultramafic sills below the Nikolai basalts. Nonetheless, the 3-D model cannot preclude the possibility of later, minor steepening of the limbs of the basin during post-Triassic collision.

[59] Although a synmagmatic sag basin was primarily responsible for development of the Amphitheater synform, preexisting structures and stratigraphic and facies boundaries below the eruptive Nikolai sequence may have played a significant role in controlling the emplacement, shape, and location of magma chambers, and the connectivity and complexity of magmatic channels, some of which eventually vented to the surface.

[60] The alignment of the axis of the Amphitheater synform, which is roughly parallel to broad folding in the Tangle Formation and to the strike of south directed thrust faults, suggests that the synform may have been steepened by Cretaceous(?) to Tertiary deformation superposed on the sag basin. The apparent incongruity of this with inferences made from recent mapping (Table 1) and from the 3-D model, may be reconciled if the deep, dense keel of the Amphitheater structure, had either locally influenced deformation of the surrounding sediments during later folding and/or rotated into the regional stress field. In summary, the geologic mapping and geophysical modeling are consistent with a sag basin model for the initial development of the Amphitheater synform with subsequent [Cretaceous(?) to Tertiary] deformation that modified the synform through broad warping, limb steepening, and possible rotation.

7. Conclusions

[61] In the Amphitheater Mountains, central Alaska Range, a major eruptive center for the subcontinental-scale Triassic Nikolai Greenstone mafic LIP forms a broad synformal structure of thick, extensive cumulate mafic and ultramafic sills and overlying Nikolai Greeenstone lavas. Because of the volume of the flood basalt and the abundance of comagmatic and layered intrusions, the Nikolai LIP in this region has the potential to host world class deposits of PGE and Ni-Cu. We undertook 3-D potential field modeling in order to better characterize the geometry of the Amphitheater synform and to constrain the extent of subsurface units that may contain deposits.

[62] We built a 3-D potential field model consisting of 11 layers, initially constructed from a set of intersecting 2-D models, and further developed through a series of forward and inverse calculations. The 3-D model confirms the presence of a deep,

keel-like, and asymmetric geometry to the synform that supports a sag basin model for development of the Amphitheater Mountains structure. The alignment of the axis of the Amphitheater synform with the trend of broad warping and folding in the Tangle Formation suggests that the orientation and form of the structure may to some extent have been modified by, or perhaps influenced, Cretaceous(?) to Tertiary deformation.

[63] The 3-D model also allows for volume calculations of potentially important mineral resource-bearing ultramafic rock units. Estimated volumes of Nikolai basalt and ultramafic rocks, derived from the 3-D model, are on the order of 1000 and 2000 km^3, respectively, substantially expanding the mineral potential of the complex.

[64] A regional geophysical assessment of Nikolai-related anomalies [*Glen et al.*, 2007a] suggests that the Nikolai LIP is far more extensive than previously known, and that the magmatic feeder system in the Amphitheater Mountains may be one segment of a much larger dissected structure, or one of several isolated or interconnected complexes occurring throughout south central Alaska.

Acknowledgments

[65] We thank Peter Bittenbender for field support and assisting in field logistics and Bob Morin for help with data reduction. We are grateful to Rick Saltus, Sarah Roeske, Warren Nokleberg, and David Ponce for their reviews and comments that helped improve the manuscript. We are also grateful to Chris Musselman for assisting with model animations.

References

Andreasen, G. E., W. J. Dempsey, J. R. Henderson Jr., and F. P. Gilbert (1958), Aeromagnetic map of the Copper River basin, Alaska, *U.S. Geol. Surv. Geophys. Invest. Map, GP-0156*, scale 1:125,000.

Andreasen, G. E., A. Grantz, I. Zietz, and D. F. Barnes (1964), Geologic interpretation of magnetic and gravity data in the Copper River basin, Alaska, *U.S. Geol. Surv. Prof. Pap., 316-H*, 135–153.

Barker, F., L. A. Sutherland Brown, J. R. Budahn, and G. Plafker (1989), Back-Arc with frontal-arc component origin of Triassic Karmutsen Basalt, British Columbia, Canada, *Chem. Geol.*, *75*, 81–102, doi:10.1016/0009-2541(89)90022-3.

Barnes, D. F. (1976), Bouguer gravity map of Alaska, *U.S. Geol. Surv. Open File Rep., 76-0070*, 1 p., 1 sheet.

Berg, H. C., D. L. Jones, and D. H. Richter (1972), Gravina-Nutzotin belt—Tectonic significance of an upper Mesozoic sedimentary and volcanic sequence in southern and southeastern Alaska, in *Geological Survey Research 1972*, *U.S. Geol. Surv. Prof. Pap., 800-D*, D1–D24.

Berg, H. C., D. L. Jones, and P. J. Coney (1978), Pre-Cenozoic tectonostratigraphic terranes of southeastern Alaska and adjacent areas, *U.S. Geol. Surv. Open File Rep., 78-1085*.

Bittenbender, P. E., K. W. Bean, J. M. Kurtak, and J. Deininger Jr. (2007), Mineral assessment of Delta River mining district area, east-central Alaska, *Tech. Rep. 57*, 676 p., Bur. of Land Manage. Alaska, Anchorage.

Blakely, R. J. (1995), *Potential Theory in Gravity and Magnetic Applications*, 441 pp., Cambridge Univ. Press, Cambridge, U. K., doi:10.1017/CBO9780511549816.

Blakely, R. J., and G. G. Connard (1989), Crustal studies using magnetic data, in *Geophysical Framework of the Continental United States*, edited by L. C. Pakiser and W. D. Mooney, *Mem. Geol. Soc. Am.*, *172*, 45–60.

Bryan, S. E., and R. E. Ernst (2008), Revised definition of large igneous provinces (LIPs), *Earth Sci. Rev.*, *86*, 175–202, doi:10.1016/j.earscirev.2007.08.008.

Burns, L. E. (2003), Portfolio of aeromagnetic and resistivity maps of the southern Delta River area, east-central Alaska, Geophys. *Rep. 2003-8*, 15 pp. State of Alaska, Dep. of Nat. Resour., Div. of Geol. and Geophys. Surv., Anchorage.

Campbell, D. L., and W. J. Nokleberg (1986), Magnetic model of a profile across northern Copper River basin, northeastern Gulkana Quadrangle, *U.S. Geol. Surv. Circ.*, *978*, 35–38.

Campbell, D.L., and W. J. Nokleberg (1997), Interpretation of aeromagnetic map and related geophysical data for Mount Hayes 1 degrees × 3 degrees quadrangle, Alaska, *U.S. Geol. Surv. Open File Rep., 97-0280*, 64 pp., 2 sheets.

Carmichael, R. S. (1982), Magnetic properties of minerals and rocks, in *CRC Handbook of Physical Properties of Rocks*, vol. 2, edited by R. S. Carmichael, pp. 229–287, CRC Press, Boca Raton, Fla.

Coffin, M. F., and O. Eldholm (1994), Large igneous provinces; crustal structure, dimensions, and external consequences, *Rev. Geophys.*, *32*(1), 1–36, doi:10.1029/93RG02508.

Connard, G. G., R. W. Saltus, P. L. Hill, L. Carlson, and B. Milicevic (1999), Alaska digital aeromagnetic database description, *U.S. Geol. Surv. Open File Rep., 99-0503*, 18 pp.

Cordell, L., and A. E. McCafferty (1989), A terracing operator for physical property mapping with potential field data, *Geophysics*, *54*, 621–634, doi:10.1190/1.1442689.

Dobrin, M. B., and C. H. Savit (1988), *Introduction to Geophysical Prospecting*, 4th ed., 867 pp., McGraw-Hill, New York.

Eastham, K. R., and K. D. Ridgway (2002), Stratigraphic and provenance data from the Upper Jurassic–Upper Cretaceous Kahiltna assemblage of south-central Alaska, in *Studies in Alaska by the U.S. Geological Survey During 2000*, edited by F. H. Wilson and J. P. Galloway, *U.S. Geol. Surv. Prof. Pap., 1662*, 45–53.

Ellis, W. T. (2000), Exploration update Ni-Cu-PGE mineralization in the Triassic of eastern Wrangellia, central Alaska Range: Alaska National Interest Lands Conservation Act (ANILCA)—20 years later, paper presented at Alaska Miner's Association 2000 Annual Convention, Anchorage, Alaska.

Ernst, R. E., and K. L. Buchan (2001), Large mafic magmatic events through time and links to mantle-plume heads, *Spec. Pap. Geol. Soc. Am.*, *352*, 483–575.

Glen, J. M. G., J. M. Schmidt, and R. Morin (2007a), Gravity and magnetic character of south-central Alaska: Constraints on geologic and tectonic interpretations, and implications for mineral exploration, in *Growth of a Collisional Continental Margin: Tectonic Growth of a Collisional Continental Margin*,

edited by K. D. Ridgway et al., *Spec. Pap. Geol. Soc. Am.*, *431*, 593–622.

Glen, J. M. G., J. M. Schmidt, L. Pellerin, D. K. McPhee, and J. M. O'Neill (2007b), Crustal structure of Wrangellia and adjacent terranes inferred from geophysical studies along a transect through the northern Talkeetna Mountains, in *Growth of a Collisional Continental Margin: Tectonic Growth of a Collisional Continental Margin*, edited by K. D. Ridgway et al., *Spec. Pap. Geol. Soc. Am.*, *431*, 21–41.

Gradstein, F. M., and J. G. Ogg (2004), Geologic time scale 2004: Why, how, and where next: Report of the International Commission on Stratigraphy, *Lethaia*, *37*(2), 175–181, doi:10.1080/00241160410006483.

Grauch, V. J. S., and L. Cordell (1987), Limitations of determining density or magnetic boundaries from the horizontal gradient of gravity or pseudogravity data, *Geophysics*, *52*, 118–121, doi:10.1190/1.1442236.

Greene, A. R., J. S. Scoates, and D. Weis (2008), Wrangellia flood basalts in Alaska; a record of plume-lithosphere interaction in a Late Triassic accreted oceanic plateau, *Geochim. Cosmochim. Acta*, *72*(12S), A326.

Greene, A. R., J. S. Scoates, D. Weis, and S. Israel (2009), Geochemistry of Triassic flood basalts from the Yukon (Canada) segment of the accreted Wrangellia oceanic plateau, *Lithos*, *110*(1–4), 1–19, doi:10.1016/j.lithos.2008.11.010.

Greene, A. R., J. S. Scoates, D. Weis, E. C. Katvala, S. Israel, and G. T. Nixon (2010), The architecture of oceanic plateaus revealed by the volcanic stratigraphy of the accreted Wrangellia oceanic plateau, *Geosphere*, *6*, 47–73, doi:10.1130/GES00212.1.

Hillhouse, J. W., and R. S. Coe (1994), Paleomagnetic data from Alaska, in *The Geology of North America*, vol. G-1, *The Geology of Alaska*, edited by G. Plafker and H. C. Berg, pp. 797–812, Geol. Soc. of Am., Boulder, Colo.

Hillhouse, J. W., and C. S. Gromme (1984), Northward displacement and accretion of Wrangellia; new paleomagnetic evidence from Alaska, *J. Geophys. Res.*, *89*(B6), 4461–4477, doi:10.1029/JB089iB06p04461.

Irvine, T. N. (1980), Magmatic infiltration metasomatism, double-diffusive fractional crystallization, and adcumulus growth in the Muskox intrusion and other layered intrusions, in *Physics of Magmatic Processes*, edited by R. B. Hargreaves, pp. 325–383, Princeton Univ. Press, Princeton, N. J.

Jones, D. L., W. P. Irwin, and A. T. Ovenshine (1972), Southeastern Alaska: A displaced continental fragment?, *U.S. Geol. Surv. Prof. Pap.*, *800-B*, B211–B217.

Jones, D. L., N. J. Silberling, and J. Hillhouse (1977), Wrangellia—A displaced terrane in northwestern North America, *Can. J. Sci. Earth*, *14*(11), 2565–2577. doi:10.1139/e77-222.

Kerr, A. C., and J. J. Mahoney (2007), Oceanic plateau: Problematic plumes, potential paradigms, *Chem. Geol.*, *241*, 332–353, doi:10.1016/j.chemgeo.2007.01.019.

Lassiter, J. C., M. T. Silk, M. A. Richards, D. J. DePaolo, C. G. Farnetani, and R. A. Duncan (1995), Constraints on the origin of the Wrangellia flood basalt province; support for the plume impact model of flood basalt formation, *Eos Trans. AGU*, *76*(46), 587.

Morin, R. L., and J. M. G. Glen (2002), Principal facts for 463 gravity stations in the vicinity of Tangle Lakes, east central Alaska, *U.S. Geol. Surv. Open File Rep., 02-0096*, 19 pp. (Available at http://geopubs.wr.usgs.gov/open-file/of02-96/.)

Morin, R. L., and J. M. G. Glen (2003), Principal facts for 408 gravity stations in the vicinity of the Talkeetna Mountains, south-central Alaska, *U.S. Geol. Surv. Open File Rep., 03-27*, 19 pp. (Available at http://geopubs.wr.usgs.gov/open-file/of03-27/.)

Naldrett, A. J., and P. C. Lightfoot (1999), Ni-Cu-PGE deposits of the Noril'sk region, Siberia; their formation in conduits for flood basalt volcanism, in *Dynamic Processes in Magmatic Ore Deposits and Their Application to Mineral Exploration, Short Course Notes*, vol. 13, edited by R. R. Keays et al., pp. 195–249, Geol. Assoc. of Can., St. Johns, Newfoundland.

Naldrett, A. J., V. A. Fedorenko, P. C. Lightfoot, V. I. Kunilov, N. S. Gorbachev, W. Doherty, and Z. Johan (1995), Ni-Cu-PGE deposits of Noril'sk region, Siberia; Their formation in conduits for flood basalt volcanism, *Trans. Inst. Min. Metall., Sect. B*, *104*, 18–36.

Naldrett, A. J., H. Keats, K. Sparkes, and S. Moore (1996), Geology of the Voisey's Bay Ni-Cu-Co deposit, Labrador, Canada, *Explor. Min. Geol.*, *5*, 169–179.

Nokleberg, W. J., J. N. Aleinikoff, I. M. Lange, S. R. Silva, R. T. Miyaoka, C. E. Schwab, and R. E. Zenher (1992), Preliminary geologic map of the Mount Hayes Quadrangle, eastern Alaska Range, Alaska, scale 1:250,000, *U.S. Geol. Surv. Open File Rep., 92-594*, 39 pp., 1 plate.

Nokleberg, W. J., G. Plafker, and F. H. Wilson (1994), Geology of south-central Alaska, in *The Geology of North America*, vol. G1, *The Geology of Alaska*, edited by G. Plafker and H. C. Berg, pp. 311–365, Geol. Soc. of Am., Boulder, Colo.

Olhoeft, G. R., and G. R. Johnson (1989), Densities of rocks and minerals, in *Practical Handbook of Physical Properties of Rock and Minerals*, edited by R. S. Carmichael, pp. 139–176, CRC Press, Boca Raton, Fla.

Panuska, B. C. (1990), An overlooked, world class Triassic flood basalt event, *Geol. Soc. Am. Abstr. Programs*, *22*(7), 168.

Plafker, G., and H. C. Berg (1994), Overview of the geology and tectonic evolution of Alaska, in *The Geology of North America*, vol. G1, *The Geology of Alaska*, edited by G. Plafker and H. C. Berg, pp. 989–1021, Geol. Soc. of Am., Boulder, Colo.

Richards, M. A., D. L. Jones, R. A. Duncan, and D. J. DePaolo (1991), A mantle plume initiation model for the Wrangellia flood basalt and other oceanic plateaus, *Science*, *254*, 263–267, doi:10.1126/science.254.5029.263.

Ridgway, K. D., J. M. Trop, W. J. Nokleberg, C. M. Davidson, and K. R. Eastham (2002), Mesozoic and Cenozoic tectonics of the eastern and central Alaska Range; progressive basin development and deformation in a suture zone, *Geol. Soc. Am. Bull.*, *114*(12), 1480–1504, doi:10.1130/0016-7606(2002)114<1480:MACTOT>2.0.CO;2.

Saltus, R. W., and G. C. Simmons (1997), Composite and merged aeromagnetic data for Alaska; a web site for distribution of gridded data and plot files, *U.S. Geol. Surv. Open File Rep., 97-0520*, 15 pp.

Saltus, R. W., T. L. Hudson, and F. H. Wilson (2007), The geophysical character of southern Alaska—Implications for crustal evolution, in *Growth of a Collisional Continental Margin: Tectonic Growth of a Collisional Continental Margin*, edited by K. D. Ridgway et al., *Spec. Pap. Geol. Soc. Am.*, *431*, 1–20.

Sanger, E., and J. M. G. Glen (2003), Density and magnetic susceptibility values for rocks of the Talkeetna Mountains and adjacent region, south-central Alaska, *U.S. Geol. Surv. Open File Rep., 03-268*, 42 pp. (Available at http://geopubs.wr.usgs.gov/open-file/of03-268/.)

Schmidt, J. M., and R. K. Rogers (2007), Metallogeny of the Nikolai large igneous province (LIP) in southern Alaska and its influence on the mineral potential of the Talkeetna Mountains, in *Growth of a Collisional Continental Margin: Tectonic Growth of a Collisional Continental Margin*, edited by K. D. Ridgway et al., *Spec. Pap. Geol. Soc. Am.*, *431*, 623–648.

Schmidt, J. M., M. B. Werdon, and B. Wardlaw (2003), New mapping near Iron Creek, Talkeetna Mountains, indicates presence of Nikolai Greenstone, in *Short Notes on Alaska Geology*, edited by K. H. Clautice, *Rep. 1*20, pp. 101–108, Alaska Div. of Geol. and Geophys. Surv., Anchorage.

Stout, J. H. (1976), Geology of the Eureka Creek area, east-central Alaska Range, *Geol. Rep. 46*, 32 pp., Alaska Div. of Geol. and Geophys. Surv., Anchorage.

Talwani, M., J. L. Worzel, and M. G. Landisman (1959), Rapid gravity computations for two-dimensional bodies with application to the Mendocino submarine fracture zone, *J. Geophys. Res.*, *64*(1), 49–59, doi:10.1029/JZ064i001p00049.

Trop, J. M., K. D. Ridgway, J. D. Manuszak, and P. Layer (2002), Mesozoic sedimentary-basin development on the allochthonous Wrangellia composite terrane, Wrangell Mountains basin, Alaska: A long-term record of terrane migration and arc construction, *Geol. Soc. Am. Bull.*, *114*, 693–717, doi:10.1130/0016-7606(2002)114<0693:MSBDOT>2.0.CO;2.

Werdon, M. B., J. R. Riehle, J. M. Schmidt, R. J. Newberry, and G. H. Pessel (2001), Geologic map of the Iron Creek area, Talkeetna Mountains B-5 quadrangle, Alaska, *Raw Data File PIR 2000-7*, 1 sheet, scale 1:63,360, Alaska Div. of Geol. and Geophys. Surv., Anchorage.